CIRCULATING COPY
Sea Grant Depository

TAMU-T-76-012 C. 2

Supplemental Lighting for Underwater Photography

A Computer Program for Design Analysis

BERNARD D. GREESON and ROBERT E. RANDALL

Ocean Engineering Program

TAMU-SG-76-212
COE Report No. 194
September 1976

TEXAS A&M UNIVERSITY SEA GRANT COLLEGE

SUPPLEMENTAL LIGHTING
FOR
UNDERWATER PHOTOGRAPHY.
A COMPUTER PROGRAM FOR DESIGN ANALYSIS

by

Bernard D. Greeson and Robert E. Randall

Ocean Engineering Program

September 1976

TAMU-SG-76-212

COE Report No. 194

Partially supported through Institutional Grant 04-5-158-19
to Texas A&M University
by the National Oceanic and Atmospheric
Administration's Office of Sea Grants
Department of Commerce

$4.00

Order from:

Department of Marine Resources Information
Center for Marine Resources
Texas A&M University
College Station, Texas 77843

ABSTRACT

Most lighting systems for underwater photography are developed through experiment. This is a costly and time-consuming process and can produce less than optimum results. The objectives of this paper are to discuss some mathematical expressions which can be used to analyze the design of an underwater lighting system, to introduce a computer program which can be used to solve these expressions by numerical techniques, and to illustrate the use of this program in the design of two hypothetical lighting arrangements.

Mathematical expressions for the image contrast, spectral radiance, and overall brightness of the light received by the camera are developed. Knowledge of the image contrast as a function of lighting arrangement allows the underwater photographer to minimize the backscattering of light from the water column. Evaluation of the spectral radiance is useful because it permits the engineer to select the optimum color correction filter for his system. Finally, the correct exposure settings can be calculated from the overall brightness of the light received by the underwater camera.

A computer program is described which numerically solves the mathematical equations for image contrast, spectral radiance, and over-all brightness for a particular lighting system. This program can be used to determine the best camera and lamp arrangement, correct camera exposure settings, and the optimum type of lamp. Therefore, the underwater lighting system can be evaluated rather inexpensively and quickly on the computer prior to an actual underwater test. Two hypothetical lighting situations are evaluated to demonstrate the capabilities of the computer program.

PREFACE

The computer program introduced in this report was developed as part of the research program in the Ocean Engineering Group of Texas A&M University.

The manuscript was edited by Dr. Gisela Mahoney and typed for publication by Mrs. Dianna M. Hofflinger.

TABLE OF CONTENTS

LIST OF TABLES

LIST OF FIGURES

FIGURE Page

SUPPLEMENTAL LIGHTING FOR UNDERWATER PHOTOGRAPHY

I. INTRODUCTION

Underwater photography is a relatively recent development in the field of oceanography. The first successful photographs of the deep sea floor were made in 1940 by Maurice Ewing and Allyn Vine of the Woods Hole Oceanographic Institution. Since then, techniques for underwater photography have developed rapidly. Multiple exposure cameras have been designed which allow several hundred exposures on a single lowering. Improved lenses, electronic strobes, and sophisticated camera positioning and triggering systems have greatly improved the quality of deep sea photographs. Despite all these innovations, underwater photography is still in its infancy. New and improved photographic systems will continue to be developed, helping to extend our knowledge of the deep sea floor.

The purpose of this paper is to develop expressions which can be used by the ocean engineer in analyzing the design of an underwater photographic system. The paper also introduces a computer program which enables him to solve these expressions numerically. In particular, the computer solution provides values for image contrast, spectral radiance, and overall brightness of the light received by the camera. Knowledge of the image contrast is important, because if this parameter can be maximized, backscattering of light from the water column will be minimal. Knowledge of the spectral radiance is also important, because it permits the engineer to select the optimum color correction filter for

his system. And finally, correct exposure settings can be calculated from the overall brightness of the light received by the underwater camera.

This paper is divided into four sections. Section I is an introduction and outlines the structure and direction of the text. Section II discusses the variation of light attenuation in the ocean, surveys absorption and single encounter scattering theory, and points out the difficulty in extending this theory to multiple scattering. Section III surveys contemporary underwater illumination equipment, introduces empirical relationships describing light transmission through water, and develops expressions which can be used to analyze the design of an underwater photographic system. Section IV presents two examples illustrating the use of these expressions.

II. LIGHT TRANSMISSION IN WATER

Oceanographic Considerations

A beam of light which has all its rays parallel is said to be "collimated". When a collimated beam of monochromatic light is passed through pure distilled water, the irradiance (or illuminance) E at a distance ℓ from the light source can be predicted by the following equation (1, 2):

$$E(\ell) = E_0 e^{-\alpha \ell} \qquad 1$$

where:
- $E(\ell)$ = the irradiance (or illuminance) at a distance ℓ from the light source due only to non-scattered light. (Units = watts/meter^2 or lumens/meter^2)
- E_0 = the irradiance (or illuminance) at the light source. (Units = watts/meter^2 or lumens/meter^2)
- α = the volume attenuation coefficient. (Units=meter^{-1})

The terms "irradiance" and "illuminance" may not be familiar. The irradiance at a point equals the radiant flux of light incident on an infinitesimal element of surface containing the point under consideration, divided by the area of that element. Illuminance may be defined in a similar manner, except here we are referring to the luminous flux instead of the radiant flux. (3, 4)

Equation 1 is deceptively simple, but it applies only for monochromatic light. In order to calculate $E(\ell)$ for polychromatic light, we must first calculate $E(\ell)$ at each component wavelength, then sum the results. This is because the attenuation of light is a complex function of wavelength. (1)

The attenuation of light is due to two independent phenomena: absorption and scattering. The term absorption refers to the various processes whereby light is converted to other forms of energy (thermal kinetic energy, chemical potential energy, and so on). Scattering refers to any process whereby the direction of the light beam is changed without a loss of energy. Thus the volume attenuation coefficient, α, can be considered to be the sum of two independent coefficients, a and s (2):

$$\alpha = a + s \qquad 2$$

where:

a = the volume absorption coefficient. (Units = $meter^{-1}$)
s = the volume scattering coefficient. (Units = $meter^{-1}$)

Measurements of the volume attenuation coefficient in pure distilled water have been made many times with varying results. The results of several investigators are plotted in Figure 1.

The first simultaneous measurements of both α and s, the volume attenuation and scattering coefficients, were made by HULBERT (1945) at the Naval Research Laboratory. This enabled him to then calculate a, the volume absorption coefficient, using Equation 2. HULBERT's values are frequently referenced and are reproduced for convenience in Table I. Minimum attenuation is noted to lie in the blue-green region, 460-470 nanometers (nm) wavelength. (5)

The attenuation of light at a given wavelength in pure distilled water is the minimum attenuation possible for light in natural water. The additional quantities of dissolved and suspended matter in natural water generally produce an increase in the absorption and/or scattering of light. (1) Some references prefer a more explicit form of Equation 2 when discussing the attenuation of light in natural water (6):

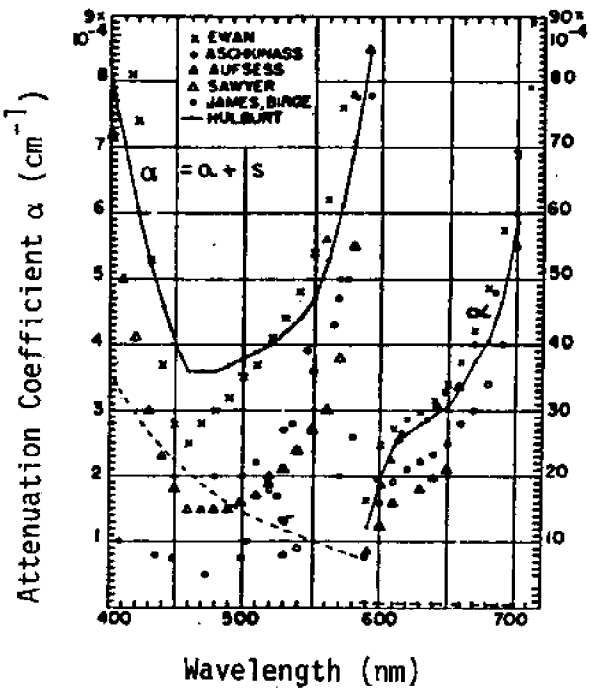

Figure 1. Absorption and scattering in distilled water. (5)

Note: For clarity the scale of the ordinate for $\alpha < 580nm$ is 10 times the scale for $\alpha > 580nm$.

TABLE I: Absorption and scattering in pure distilled water. [according to HULBERT (1945).] (5)

Wavelength (nm)	α (m^{-1})	a (m^{-1})	s (m^{-1})
400	8.0×10^{-2}	4.4×10^{-2}	3.57×10^{-2}
410	7.0	3.8	3.23
420	6.1	3.1	2.95
430	5.3	2.6	2.69
440	4.6	2.1	2.45
450	4.0	1.7	2.25
460	3.6	1.6	2.04
470	3.6	1.7	1.89
480	3.65	1.8	1.72
490	3.7	2.1	1.59
500	3.8	2.3	1.47
510	3.9	2.6	1.35
520	4.0	2.8	1.25
530	4.2	3.0	1.17
540	4.4	3.3	1.09
550	4.7	3.7	1.00
560	5.3	4.4	0.932
570	6.6	5.7	0.868
580	8.4	8.6	0.810
590	12.0	11.2	0.756
600	19.7	19.0	0.708
610	24.3	23.6	0.662
620	26.5	25.9	0.618
630	28.0	27.4	0.581
640	29.2	28.7	0.535
650	30.8	30.3	0.507
660	33.5	33.0	0.483
670	37.5	37.0	0.455
680	40.6	40.2	0.429
690	46.7	46.3	0.404
700	57.6	57.2	0.380

$$\alpha_\lambda = a_\lambda + a_{w\lambda} + s_\lambda + s_{w\lambda} \qquad 3$$

where:

α_λ = the volume attenuation coefficient for monochromatic light of wavelength λ . (Units = meter^{-1})

a_λ , s_λ = the volume absorption and scattering coefficients for monochromatic light of wavelength λ in pure water. (Units = meter $^{-1}$)

$a_{w\lambda}$, $s_{w\lambda}$ = the volume absorption and scattering coefficients due to suspended and dissolved matter in natural water for monochromatic light of wavelength λ . (Units = meter^{-1})

However, since it is presently impractical to measure $a_{w\lambda}$ and $s_{w\lambda}$ directly, Equation 2 is in more common use. (3, 7)

The attenuation of light by seawater (as a function of wavelength) has been measured at various locations by a number of observers. An excellent account of early work in this field can be found in the classic work on oceanography, H.U. SVERDRUP et al., The Oceans (1942). Based on data by UTTERBACK (1936) and JORGENSEN and UTTERBACK (1936), SVERDRUP et al. prepared a plot of "extinction coefficients per meter" for oceanic and coastal waters of minimum, average, and maximum turbidity. This plot is reproduced as Figure 2. (8)

It should be pointed out that the "extinction coefficient" used by SVERDRUP et al. (1942) differs from the volume attenuation coefficient of Equation 1. The extinction coefficient (denoted by k) is a measure of the rate at which downward-traveling radiation decreases with depth. This radiation includes diffuse (or scattered) light, unlike the purely direct (or unscattered) radiation described by Equation 1. Hence, in most natural waters the extinction coefficient is smaller than the attenuation coefficient by a factor of approximately 2 or 3, with a mean ratio of approximately 2.7:1. The extinction coefficient is also referred to in some literature as the "diffuse attenuation coefficient". (1)

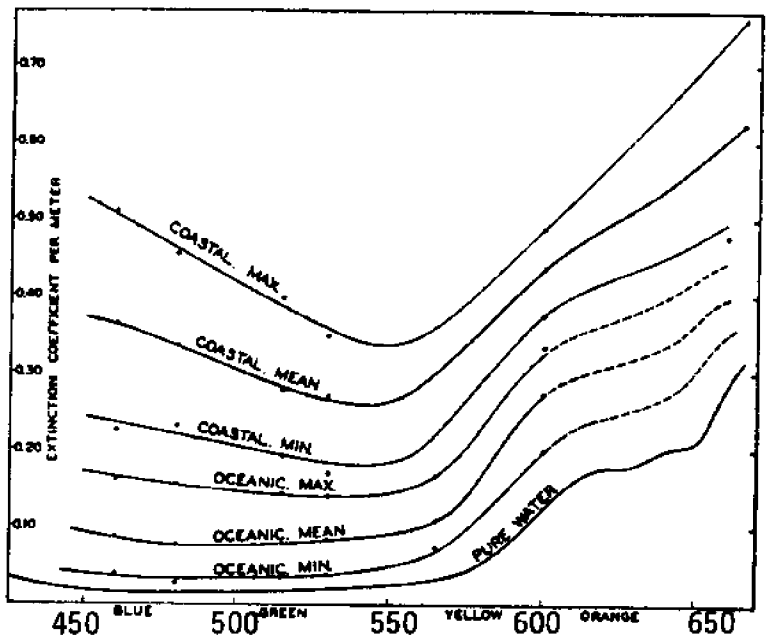

Figure 2. Extinction coefficients of radiation at different wavelengths in pure water and in different types of sea water. (8)

Examination of Figure 2 reveals a number of interesting points. In the clearest ocean water extinction coefficients appear to be about twice those in pure water, whereas in the more turbid areas of the open sea the extinction coefficient may be up to ten times as high. In coastal water the extinction coefficients may be as much as thirty or forty times those observed in pure water. Moreover, with increasing turbidity of oceanic water and especially for coastal water the attenuation at shorter wavelengths becomes more significant, producing a shift in the wavelength of minimum attenuation towards the yellow-green portion of the spectrum. Minimum attenuation for the open ocean is seen to occur at about 470-480 nm, whereas in turbid coastal water the wavelength of minimum attenuation is about 550 nm. This shift is widely attributed to (so called) "yellow substances" which may be present in coastal water. These substances are dissolved organic decomposition products (humic acids, melanoidins, etc.) which absorb strongly in the blue region of the spectrum. Results similar to Figure 2 have been obtained in various parts of the world by other observers. (8, 9)

Not only does the attenuation of light vary with water type and location, it is also a function of water depth. This is because oceanic water is not homogenous and tends to form strata. Of particular importance is the presence of plankton, living and dead, which scatter light and produce attenuation. This influence is most apparent in the mixed layer of the sea. Figure 3 illustrates several typical profiles of the attenuation coefficient as a function of depth. Below the main thermocline, clearer water generally exists. This deeper water may be optically uniform for tens or hundreds of meters. (1, 2)

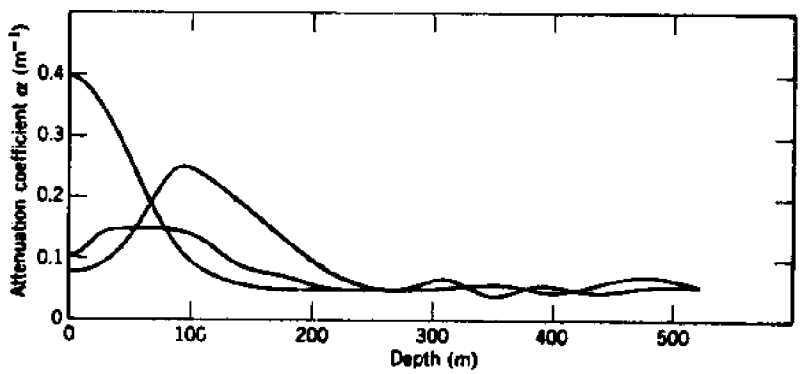

Figure 3. Several typical profiles of attenuation coefficient α as a function of depth for deep oceanic areas. (1)

Knowledge of the absorption and scattering characteristics of the water in which photography is to be attempted is essential if satisfactory results are to be attained. Since attenuation characteristics vary spatially and temporarily in all natural water, in situ measurements are preferred (1).

Absorption and Scattering Theory

Pure distilled water has very strong absorption in the infrared and ultraviolet regions of the spectrum. Measurements in the near infrared spectrum by CURIO and PETTY (1951) show five prominent absorption bands near 760, 970, 1190, 1450, and 1940 nm, and generally increasing absorption with increased wavelength. Their results are reproduced in Figure 4. (10) Earlier measurements in the ultraviolet spectrum by DAWSON and HULBERT (1934) are reproduced in Figure 5. (11)

The strong absorption noted in the infrared and ultraviolet regions of the spectrum is caused by characteristic resonances of the water molecule at these wavelengths. The infrared resonances are due to molecular excitation, and are particularly strong since water molecules are electrically polarized. The ultraviolet resonances are due to electron excitation. Even though the peak resonances are outside the visible region, these resonances are very broad band and strongly affect adjacent portions of the visible spectrum. (1) Except in the blue region of the spectrum, absorption is overwhelmingly the predominant factor limiting light transmission in clear water. (2)

The absorption of light by pure distilled water at a given temperature is solely a function of wavelength. Surprisingly, a recent investigation by SULLIVAN (1963) has shown that this function is essentially the same for artificial seawater. (12) The obvious conclusion is that sea salts exert little influence on light absorption. Unfortunately, the presence of other dissolved and suspended matter in seawater tends to increase the absorption of light, particularly at shorter wavelengths. The influence of "yellow substances" in coastal water (discussed earlier) is representative. (3)

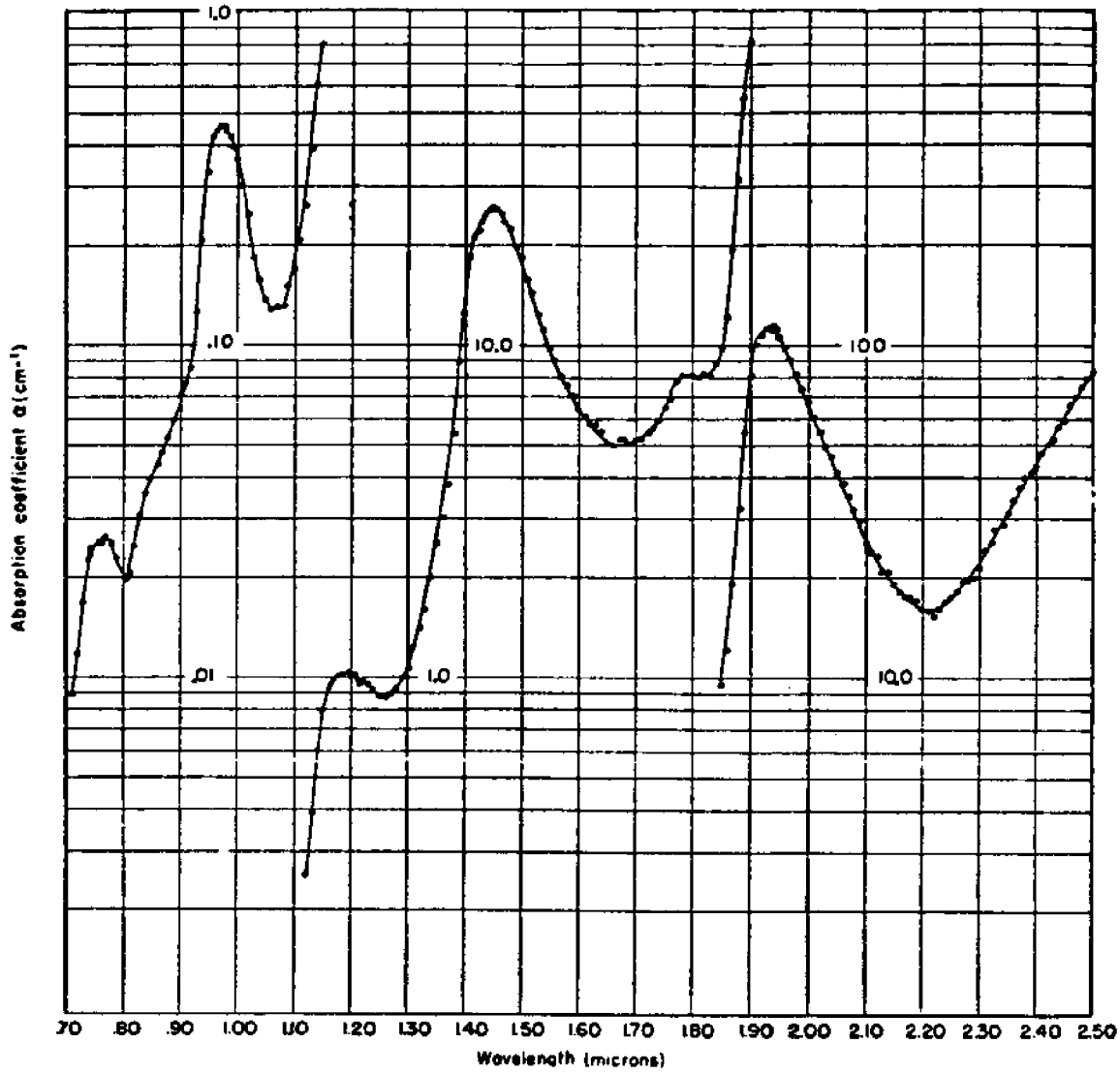

Figure 4. Absorption coefficients of water in the near infrared spectrum at 20°C. (10)

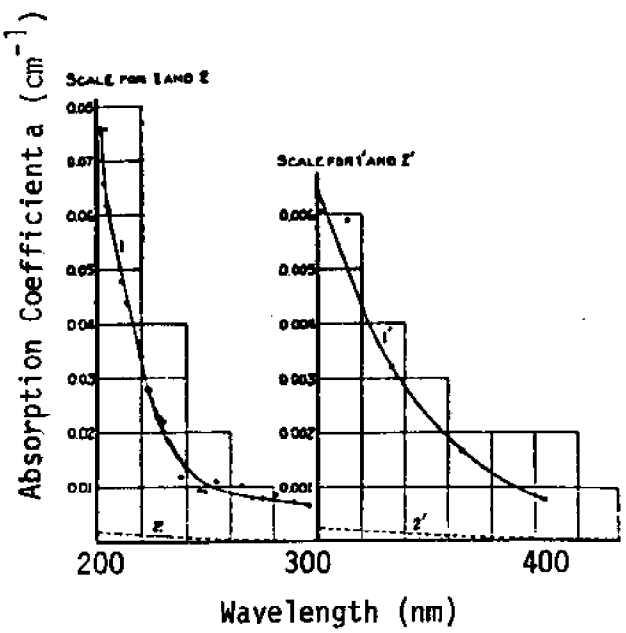

Figure 5. Ultraviolet absorption coefficient of water, curves 1 and 1' observed, curves 2 and 2' calculated from molecular scattering. (11)

Light scattering in pure distilled water can be considered to be a problem in water-molecule scattering. An approach to this problem was first introduced by Lord Rayleigh in the late nineteenth century. Although strictly applicable only to gases, the Rayleigh Theory predicts that the scattering will be proportional to the inverse fourth power of the incident wavelength. (3, 13, 14) More explicitly (1):

$$S_R = \frac{8}{3} (N \pi r^2) \frac{(n^2 - 1)}{(n^2 + 2)} \frac{(2 \pi r)^4}{\lambda^4} \qquad 4$$

where: S_R = the Rayleigh scattering coefficient.
N = the number of particles (molecules) per cubic meter.
n = the index of refraction of the particle at wavelength λ.
r = the radius of the particle.
$N \pi r^2$ = the equivalent geometric cross section of the particles in a cubic meter.

It should be pointed out that the Rayleigh Theory and all subsequent theories discussed in this section attempt to predict the initial (first encounter) scattering of a light ray. Multiple scattering will be discussed at the end of Section II.

A different approach to the scattering problem was taken by Smoluchowski and Einstein in the early twentieth century. Their theory attributed light scattering to density or concentration fluctuations of small amplitude, such as are found in pure distilled water. Their results confirmed Rayleigh's conclusion that scattering is proportional to λ^{-4}. Moreover, they confirmed the symmetrical shape of the scattering diagram (3, 14) and the approximate magnitudes predicted by his theory. (1)

Calculated Rayleigh scattering coefficients are only a few percent of the observed volumetric scattering coefficients for distilled water samples. This is probably due to the fact that even elaborately prepared distilled water samples show suspended particulate matter when examined closely

under a light beam. It is unlikely that true Rayleigh scattering by optically pure water has ever really been observed. (1, 2, 5)

In natural seawater the sizes of scattering particles vary over a tremendous range. When the sizes of these particles approach the wavelengths of visible light, a complex scattering relationship exists. A theoretical approach to this problem based on electromagnetic theory was developed by Mie in 1908. In its most elemental form, Mie's results predict a scattering coefficient (1, 3):

$$S_M = N\pi r^2 K_s \qquad 5$$

where: S_M = the Mie scattering coefficient.
N = the number of particles per cubic meter.
r = the radius of the particle.
πr^2 = the equivalent geometric cross section of the particles in a cubic meter.
K_s = the efficiency factor or effective area coefficient.
K_s = the ratio of the actual scattering cross-sectional area to the geometric cross-section area.

Mie's solution for K_s involves the ratio r/λ, the index of refraction (n) of the particle, and Bessel functions. Figure 6 illustrates the general shape of Mie's solution. For $r/\lambda \ll 1$, Mie's solution is identical with Rayleigh scattering. Near the resonance region where $r/\lambda = 1$, K_s for natural water is approximately equal to 4. At larger values of r/λ, K_s fluctuates about the value 2, and at very large values of r/λ, geometric optics are approached, and K_s is near unity. For indices of refraction larger than that of water (n=1.34), the peak value of K_s is larger and occurs at a lower value of r/λ. (1, 3, 13)

Experimental observations with various sizes of quartz, flint, and diamond dust in water have tended to confirm the Mie Theory. These measurements have suggested that the scattering coefficient is proportional to the concentration of particles, and that K_s approaches the value 2 for

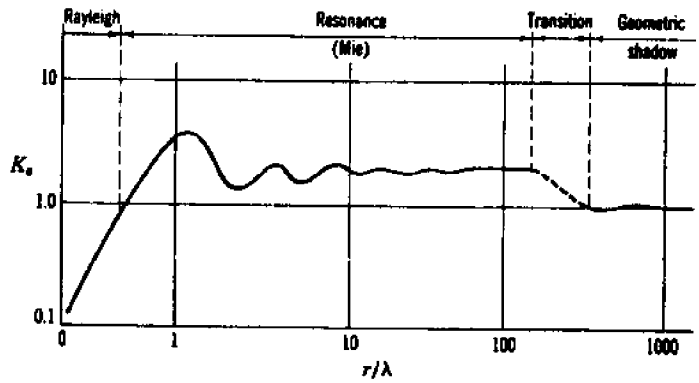

Figure 6. Approximate variation of K_s as a function of ratio r/λ . (1)

large particles. (3) Observations of light scattering by an aerosol mist have been similar. (13)

Because the ocean contains such a wide range of particle sizes, the scattering cross section for light is virtually independent of wavelength. While the sky owes its blue color to the λ^{-4} effect of Rayleigh scattering, clear ocean water is blue almost entirely due to selective absorption by the water molecules. (2)

Angular Distribution of Scattered Light

Consider a small volume of scattering material dV illuminated by a collimated beam of light. The intensity of light scattered by volume dV will (in general) be a function of spherical coordinates θ and ϕ. However, if θ and ϕ are measured as illustrated in Figure 7, the scattered light intensity will be a function of only θ. Then the total scattered light energy dF_s produced by volume dV is:

$$dF_s = S\ dV\ E(\ell) \qquad 6$$

where: S = the volume scattering coefficient.
$E(\ell)$ = the incident illumination. (Units = lumens/meter^2)

The luminous intensity per steradian which is produced by the scattering of incident light $E(\ell)$ in volume dV is termed dI. Integration of dI over 4π steradians must equal dF_s. Hence:

$$2\pi \int_0^{\pi} dI\ (\theta)\ \sin\theta\ d\theta = dF_s \qquad 7$$

Solving Equations 6 and 7 for S, the volume-scattering coefficient, yields:

$$S = 2\pi \int_0^{\pi} \frac{dI\ (\theta)}{dV\ E(\ell)}\ \sin\theta\ d\theta \qquad 8$$

Introducing the volume-scattering function $\sigma\ (\theta)$, defined as:

$$\sigma\ (\theta) \equiv \frac{dI\ (\theta)}{dV\ E(\ell)} \qquad 9$$

yields the definition for S, the volume-scattering coefficient (1):

$$S \equiv 2\pi \int_0^{\pi} \sigma(\theta)\ \sin\theta\ d\theta \qquad 10$$

The physical meaning of S has been discussed earlier in connection with Equation 2. The volume-scattering function $\sigma\ (\theta)$ may be interpreted as the fraction of the beam of light which has been scattered per unit volume of water per unit solid angle in the direction θ. (5)

It can be shown from Equations 4 and 10 that the volume-scattering function for Rayleigh scattering of unpolarized light is:

$$\sigma_R(\theta) = \frac{3}{16\pi} S_R\ (1 + \cos^2\theta). \qquad 11$$

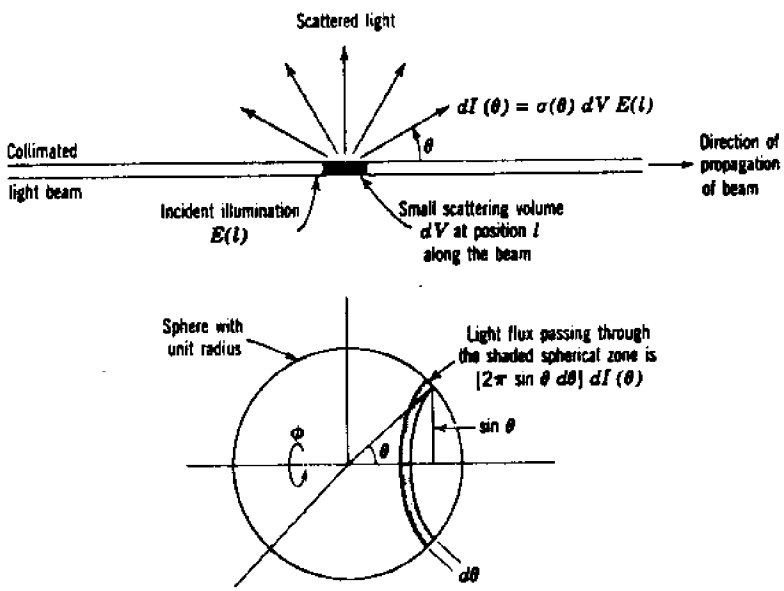

Figure 7. Volume-scattering function $\sigma(\theta)$. (1)

Figure 8 is a polar plot of $\sigma_R(\theta)$. As can be seen from the plot, forward and backward scattering are equal and are twice the scattering at 90°. (1) Experiment has shown, however, that this is not exactly correct for water molecule scattering. Anisotropy of the scattering molecules has been suggested as a likely cause, and DAWSON and HULBERT (1941) have proposed using the factor $(1+0.835\ \cos^2\theta)$ to correct for this anomaly. (14, 15)

Even in the clearest blue ocean water Rayleigh scattering consitutes only about 7% of the total scattering coefficient. However, it is the dominant factor at scattering angles near 90°, where it produces over 67% of the scattered intensity. (2)

When the sizes of the scattering particles approach or exceed the wavelengths of the incident light, Mie scattering will dominate. Scattering functions computed from the Mie Theory are extremely complex; figure 9 illustrates the results of two such calculations. The oscillatory trend in both curves is typical for a disperse suspension of non-absorbing spheres of the same radius (monodisperse suspension). If a wide range of particle sizes is present (polydisperse suspension), then the oscillatory features will be virtually absent. Such is the case in natural seawater. (3)

In situ measurements of the scattering function for natural sea water have been made at various locations around the world. Figure 10 presents observations made in lake water, coastal water, Atlantic surface water, Pacific near-coastal water, Mediterranean and Sargasso Sea water. Although a wide range of turbidity is represented, the curves are remarkably similar in shape. Each exhibits extremely strong forward scattering,

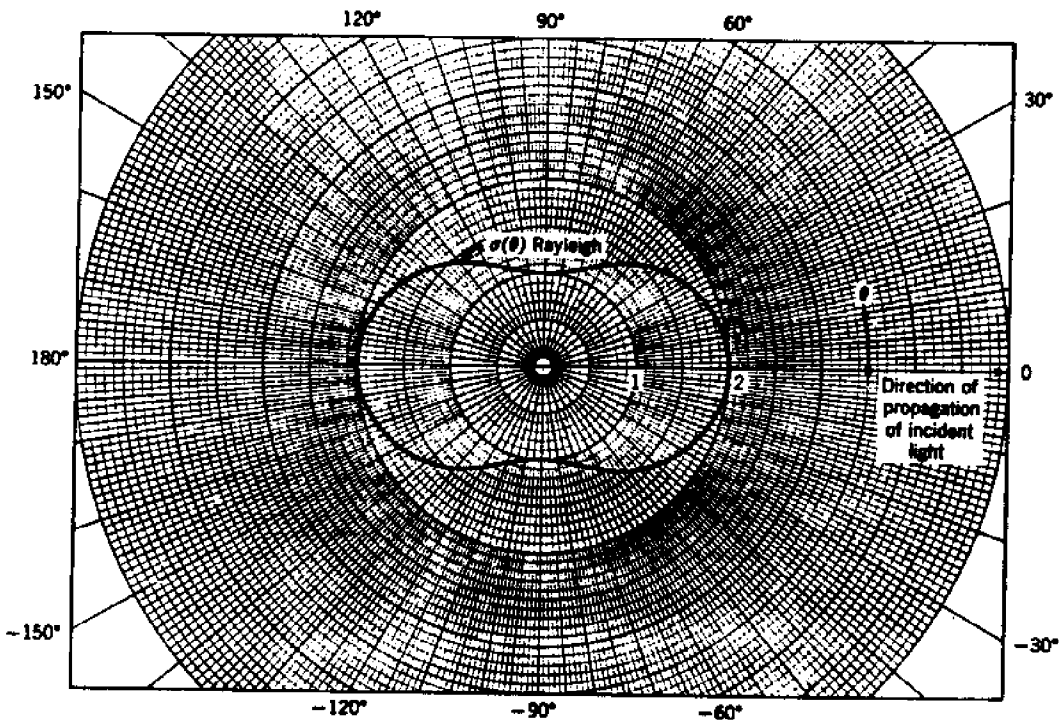

Figure 8. Polar plot of the volume-scattering function in the Rayleigh region (relative magnitude as a function of scattering angle). (1)

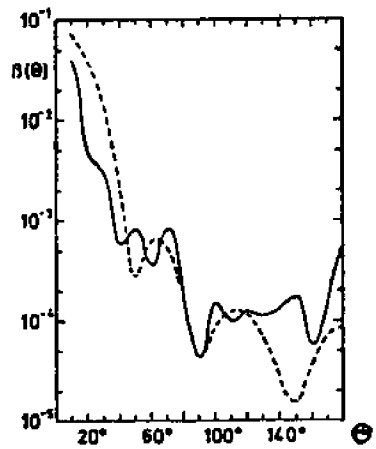

Figure 9. Scattering functions computed from the Mie theory for non-absorbing spheres with n=1.20 and r/λ = 4.77 (continuous line) (after ASHLEY and COBB, 1958), and with n = 1.15 and r/λ = 0.80 (dashed line) (after PANGONIS and HELLER, 1960.). (3)

many orders of magnitude greater than the backscatter or side scatter. (16) This marked contrast is illustrated in polar coordinates by Figure 11. (1)

An interesting analysis of the forward scattering phenomenon has been presented by MERTENS (1970). He begins by reasoning that most of the light scattering in natural water is done by transparent particles with indices of refraction near that of water. Many of these are planktonic flora and fauna whose shape is nearly spherical. Inorganic particles, on the other hand, can have indices of refraction on the order of 1.15-1.20. Mertens assumes that these particles are also nearly spherical in shape, due perhaps to abrasion with adjacent particles. Under these assumptions, he then calculates the scattering function for spherical particles with indices of refraction equal to 1.23, 1.34, and 1.43.

Mertens arrives at a number of conclusions. First, he finds that forward scattering is predominant in the two cases where there is a relatively large difference in refractive index ($\Delta n=0.1$), and even more dominant in the case where $n=1.34$ ($\Delta n=0.01$). Second, he concludes that the shape of the scattering function does not depend on the size of the scattering particles but does depend on the differences in refractive index. As the refractive difference becomes small, the shape of the scattering function approaches an asymptotic form, but more rapidly in the backscattering region than for forward scattering. Forward scattering is maximum for spherical particles when $\Delta n \approx 0$. Finally, Mertens concludes that the overall scattering attenuation level is primarily a function of the differences in refractive index and the total cross-sectional area

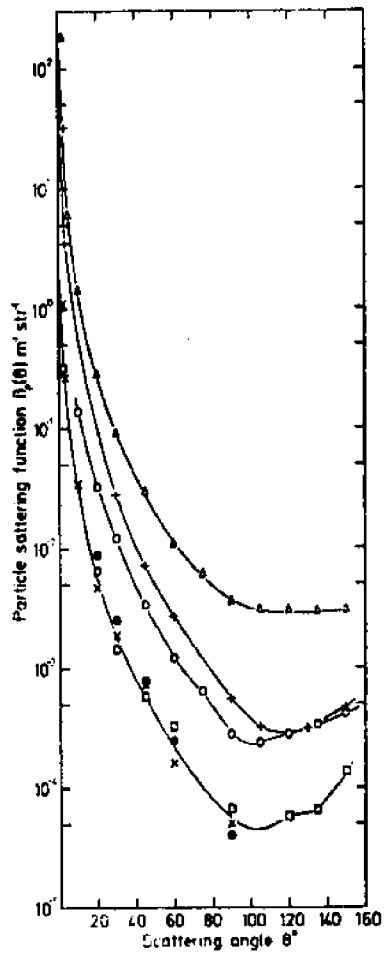

Figure 10. Particle scattering functions observed in situ (16):

Δ Duntley, lake, 1963;
o Jerlov, Atlantic, 1961;
+ Kullenberg, Baltic, 1969;
x Kullenberg, Saragasso Sea, 1968;
□ Kullenberg and Berg Olsen, Mediterranean, 1972;
• Tyler, Pacific, 1961.

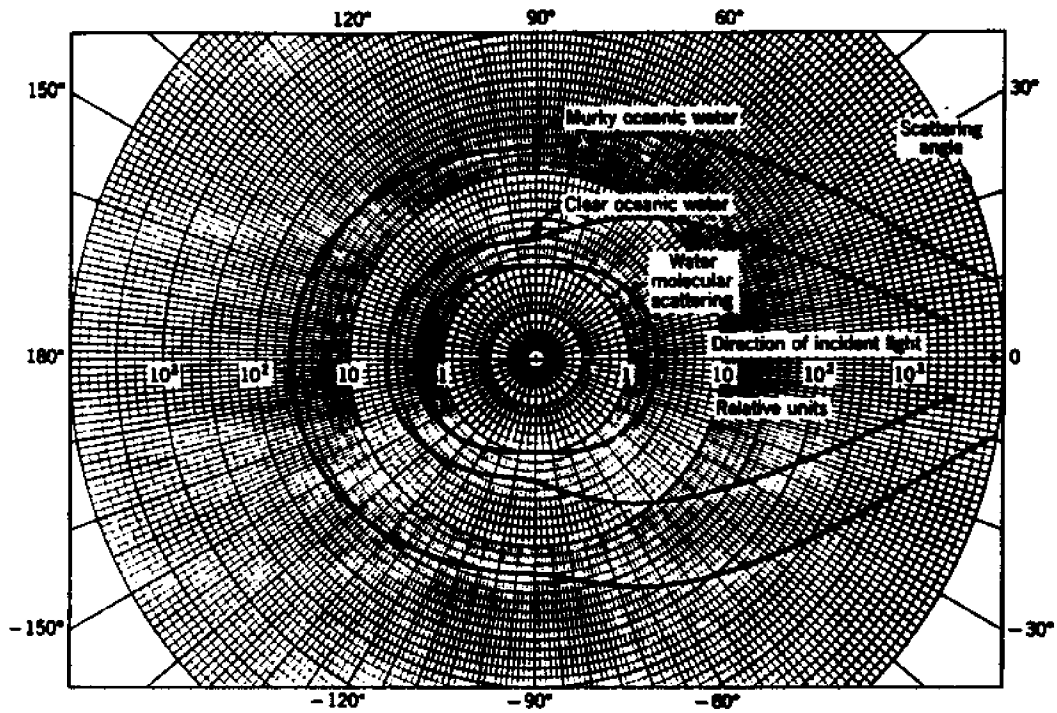

Figure 11. Polar plot of the volume-scattering functions $\sigma(\theta)$ of pure water and oceanic water. (1)

of the particles per unit volume. Size distribution is of secondary importance. (1)

Multiple Scattering

The preceding discussion has presented a relatively complete theory for single (first encounter) scattering or for scattering by small volumes of water. Unfortunately, analysis of light transmission in the ocean is complicated by the existence of multiple scattering. Light from an underwater source may be scattered many times before being absorbed. Each scattering element scatters light in accordance with its own volume-scattering function $\sigma_i(\theta)$, but some light is scattered in every direction. Thus, each small volume of the ocean receives some illumination from every other small volume. Theoretically, one could integrate this multiple scattering over the entire water column and predict total light transmission from one point to another. However, this integration would be tedious and time-consuming (at best), and hence it is rarely attempted. Although other analytical treatments of multiple scattering have been suggested (17), no fully practical solution has ever been obtained. For these reasons, the analytical approach is usually abandoned in favor of the empirical. (1, 2) Section III of this paper introduces a semi-empirical approach.

III. UNDERWATER LIGHTING SYSTEMS

Sources of Illumination

Almost all underwater photography requires some supplemental lighting. Artificial illumination is required in the deep sea just to achieve an adequate light level for photographic exposure. In more shallow water, supplemental lighting may be used to raise the illumination level enough to permit photography, or to modify the color balance and enhance image contrast. Only in very shallow water is supplemental lighting optional.

A wide variety of underwater lighting systems are available. Continuous lights are required for motion picture and television applications, and many types of incandescent and arc lamps are suitable for this purpose. Tungsten filament lamps are relatively cheap to operate and can provide light with a spectral distribution satisfactory for color photography. Tungsten-halogen lamps are an improved version which are more compact and have a nearly constant light output throughout their useful life. Arc lamps are very efficient light sources but require a more complex installation. Mercury vapor and thallium iodide lamps have dominant light components in the blue-green region of the spectrum, and these lamps are excellent for black-and-white photography and television application. Xenon, high-pressure sodium vapor, and dysprosium-thallium iodide lamps have broader and more continuous spectral distribution. With proper filtering, these lamps are suitable for color photography.

Flash sources are widely used for still photography. There are two types: expendable photoflash lamps and electronic flashtubes. Flash sources are much more compact than continuous sources and are very economical in the use of electrical power. The spectral characteristics of these lamps are generally excellent for color photography. (1, 18) Additional information on underwater lamps can be found in references 4, 19 20 and 21.

Illumination Analysis

To an underwater observer, a uniform spherical lamp emitting a divergent flux will appear to be surrounded by a glow of scattered light. As the lamp recedes, this halo will become more prominent, until at a distance of about 18 to 20 attenuation lengths (one attenuation length = $1/\alpha$), the lamp image will disappear entirely, and only the glow will be visible. Depending upon the lamp intensity and water characteristics, this residual glow will be visible for a much greater distance than predicted by Equation 1. This phenomenon is due to the existence of multiple scattering.

DUNTLEY (1963) measured the brightness of lamp images in a series of photographs taken of a receding spherical underwater lamp. He concluded that the radiance of the lamp image was attenuated exponentially in accordance with Equation 1. In other words, images are formed by light transmitted without scattering. DUNTLEY then measured the radiance of the glow surrounding the image, and his results are reproduced as Figure 12. According to DUNTLEY, "the irradiance on any surface of the target facing the lamp can be computed from these curves and, if the reflectance and gloss characteristics of the target surfaces are known, the inherent radiance of the target in any specified direction can be calculated." (2,9)

The term "radiance" may not be familiar. The radiance of a surface in a given direction is equal to the radiant intensity of the surface in that direction, divided by the projected area of the surface, as viewed from that direction. Radiance has the dimensions of watts/steradian-square meter. The term "luminance" can be defined in a similar manner, except here we are referring to luminous intensity instead of radiant intensity. (3,4)

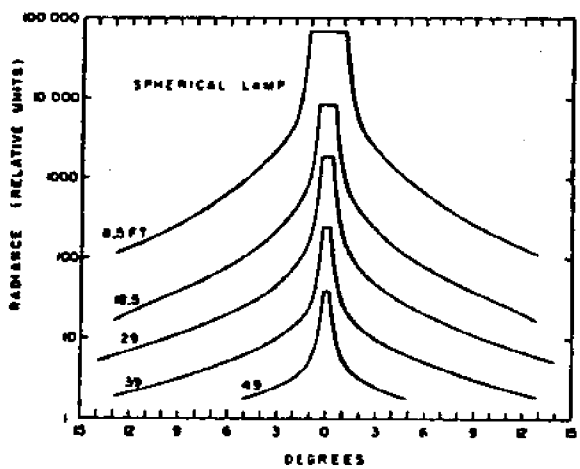

Figure 12. Angular distribution of the radiance produced by a uniform, spherical underwater lamp at distances of 8.5, 18.5, 29, and 39 feet. Attenuation length was 5.1 ft (2).

The illumination incident on any underwater object can be considered to be composed of a direct, or nonscattered component, and a component due to scattered light:

$$E(\ell) = E_D(\ell) + E_s(\ell) \qquad 12$$

where: $E(\ell)$ = the illuminance at a distance ℓ from the source.
$E_{D(\ell)}$ = the direct component of the illuminance $E(\ell)$.
$E_{s(\ell)}$ = the scattered component of the illuminance $E(\ell)$.

(Units = lumens/meter^2)

For monochromatic illumination produced at normal incidence:

$$E_D(\ell) = \frac{I}{\ell^2} e^{-\alpha \ell}$$

where: I = the intensity of the source in the direction under consideration. (Units=lumens/steradian)

Evaluation of $E_s(\ell)$ is more difficult. Based on his work with uniform spherical lamps, DUNTLEY (1963) has proposed using the following semi-empirical relationship:

$$E_s(\ell) = 2.5(1+7e^{-K\ell}) \frac{IKe^{-K\ell}}{4\pi\ell} \qquad 14$$

where: K = an attenuation coefficient for scattered light. (Units = meter^{-1})

However, few underwater lamps can be considered as uniform spherical sources of divergent light, and most emit light in patterns which are roughly conical. For these lamps, DUNTLEY (1963) recommended the following (modified) form of Equation 14:

$$E_s(\ell) = (2.5\text{-}1.5\log_{10}\frac{2\pi}{B})[1+7\left(\frac{2\pi}{B}\right)^{0.5} e^{-K\ell}]\frac{IKe^{-K\ell}}{4\pi\ell} \qquad 15$$

where: B = the beam width of the light source. (Units = radians)

Figure 13 compares the direct and scattered components of illumination from a point source of monochromatic light for a typical case where the α/K ratio is 2.7. It can be seen that the direct component is predominant when the distance to the lamp is less than about 1.8 attenuation lengths. At greater distances the scattered component exceeds the direct component, and this margin increases with increasing distance to the lamp.

Figure 13 also illustrates the scattered component of illumination from a spherical lamp which has been mounted in a blackened enclosure designed to limit its emittance to a conical beam 22.5° wide. As predicted by Equation 15, the scattered component from this lamp is less than that from the unemcumbered spherical lamp, particularly at longer ranges. For example, at 10 attenuation lengths, the scattered illumination is only about 40% of that from the bare spherical lamp. This is because each portion of the beam from the spherical lamp contributes some illumination to the point of interest.

If the spherical lamp were to be mounted in an enclosure having a mirror and lens assembly which concentrated all the light into a conical beam 22.5° wide, then the radiant intensity would theoretically be increased by a factor of about 128. However, the net increase at a distance of 10 attenuation lengths will be only about 52, for the reason discussed above. Moreover, since most underwater reflectors have efficiencies of only 30 to 60%, the net increase at 10 attenuation lengths could be as low as 15. (1,2)

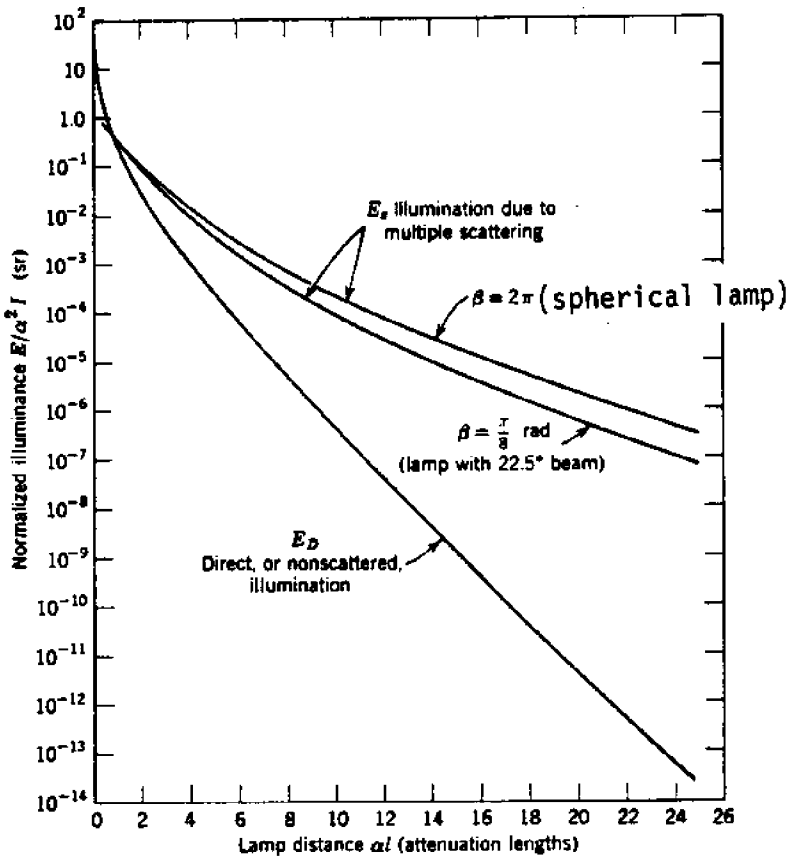

Figure 13. Direct and scattered illumination from a point source of monochromatic light in water for $\alpha / K = 2.7$.(1)

Application to Underwater Photography

Figure 14 illustrates a typical underwater photographic situation. For practical considerations, most supplemental lighting sources will be located near (but preferably not adjacent to) the underwater camera. Generally the light to subject distance will approximate the camera to subject distance, and these distances will be at most one attenuation length. Reference to Figure 13 indicates that the subject will be illuminated chiefly by direct light from the lamp. This component can be calculated from Equation 13. If the scattered light component is also considered, then the total illumination produced by the lamp near the center of the beam will be equal to the sum of Equations 13 and 15. This sum can be written in the following form (1):

$$E(L) = \frac{I}{L^2}\left[e^{-\alpha L} + c_1 KL e^{-KL} + C_2 KL e^{-2KL}\right] \qquad 16$$

where: $c_1 = (2.5 - 1.5 \log_{10} \frac{2\pi}{B}) \frac{1}{4\pi}$

$$c_2 = (2.5 - 1.5 \log_{10} \frac{2\pi}{B}) \frac{7}{4\pi}\left(\frac{2\pi}{B}\right)^{0.5}$$

$$= \left(\frac{2\pi}{B}\right)^{0.5} 7 c_1$$

In most cases, the subject being photographed can be treated as a diffuse reflector. A reflector of this type "redistributes the light incident upon it in such a manner that, whatever is the directional distribution of the incident light, the light reflected from each surface element obeys the cosine law. The surface thus appears equally bright in all directions." (4) This concept can be expressed mathematically as follows:

$$E_A(L,\phi) = \frac{(C_3)}{\pi} E(L) \cos \phi \qquad 17$$

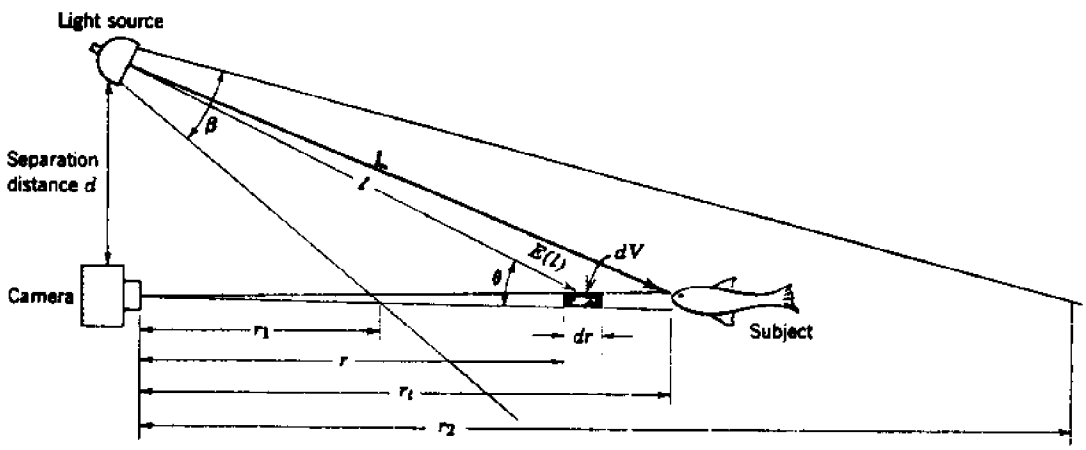

Figure 14. Light source and camera geometry. (1)

where: $E_A(L,\phi)$ = the luminance of the subject in direction ϕ, where angle ϕ is measured from the reflector surface normal. (Units = lumens/steradian - meter^2)

C_3 = the reflectivity of the diffuse reflector. (0 - 1, Units = dimensionless)

The luminance of the subject at the location of the camera (due to reflected light of wavelength λ) can be calculated from the following relationship:

$$E_A(L, \phi, r_t) = \frac{(C_3)}{\pi} E(L) \cos \phi \; e^{-\alpha r_t} \qquad 18$$

If the intensity I of the source is expressed in units of watts/steradian-nanometer, then the units of $E_A(L, \phi, r_t)$ become watts/steradian-square meter-nanometer, and solution of Equation 18 at several wavelengths between 400 and 700 nanometers will yield the spectral distribution of the subject radiance at the location of the camera. Knowledge of this spectral distribution is of value to the ocean engineer, because it allows him to predict the spectral correction necessary for balanced color photography.

Total subject luminance at the location of the camera can be calculated as follows (1):

$$B_A(L, \phi, r_t) = \int_{400nm}^{700nm} E_A(L,\phi, r_t) \, L(\lambda) \, d\lambda \qquad 19$$

where: $B_A(L, \phi, r_t)$ = the subject luminance at the location of the camera due to the light source. (Units = lumens/steradian-meter^2)

$L(\lambda)$ = the sensitivity of the receiver as a function of wavelength. (Units = lumens/watt)

For most applications, $L(\lambda)$ should be the standard luminosity curve. This curve has been adopted by the International Commission on Illumination as representing the relative capacities of radiant flux of various wavelengths to produce visual brightness sensations in the standard observer. (4)

Figure 18 illustrates the standard luminosity curve. Knowledge of the total subject luminance is also of value to the ocean engineer, because it allows him to predict required camera exposure using the following empirical relationship:

$$B = \frac{Kf^2}{(ASA)t} \qquad 20$$

where:
- B = average scene brightness (or luminance).
- f = effective aperture number of the camera.
- ASA = ASA exposure index for the film.
- t = exposure time in seconds.
- K = a constant between 10.8 and 14.5 when B is expressed in lumens/steradian-meter^2.

Strong backscattering from suspended matter in the light beam is potentially the most serious problem encountered by the user of supplemental lighting. Backscattered light can mask the image and totally ruin an underwater photograph. The luminance of a photographic subject relative to its background is called "apparent contrast" or "image contrast." (1) An analysis of the reduction in apparent contrast caused by absorption and scattering in an arbitrary medium was presented by DUNTLEY, BOILEAU, and PREISENDORFER (1957). (22) When adapted to the underwater photographic situation depicted in Figure 14, the equations of Reference 18 become:

$$C = \frac{Bt - Bb}{Bb} \qquad 21$$

where:
- C = the apparent contrast of the subject (image contrast).
- Bt = the apparent luminance of the subject at the location of the camera.
- Bb = the apparent luminance of the background at the location of the camera. (Units of Bt, Bb = lumens/steradian-meter^2)

The apparent luminance of the subject at the location of the camera has a component due to direct light from the subject and a component due to the luminance of the line of sight from r_1 to the subject (r_t):

$$Bt = B_A(L, \phi, r_t) + B_B(r_1, r_t) \qquad 22$$

where: $B_B(r_1, r_t)$ = the luminance of the line of sight from r_1 to r_t at the location of the camera. (Units = lumens/steradian-meter^2)

The apparent luminance of the background at the location of the camera has a component due to the luminance of the line of sight from the subject (r_t) to r_2 and a component due to the luminance of the line of sight from r_1 to the subject (r_t):

$$Bb = B_B(r_t, r_2) + B_B(r_1, r_t) \qquad 23$$

where: $B_B(r_t, r_2)$ = the luminance of the line of sight from r_t to r_2 at the location of the camera. (Units = lumens/steradian-meter^2)

Substituting Equations 22 and 23 into Equation 21 yields:

$$C = \frac{B_A(L, \phi, r_t) - B_B(r_t, r_2)}{B_B(r_1, r_2)} \qquad 24$$

where: $B_B(r_1, r_2) = B_B(r_1, r_t) + B_B(r_t, r_2)$

Solution of Equation 24 yields the apparent contrast of the subject for the photographic situation depicted by Figure 14. If the photographic geometry can be adjusted to maximize apparent contrast, then backscattering will be minimal. (1, 2)

Solution of Equation 24 is not difficult, but it does require expressions for $B_B(r_1,r_2)$ and $B_B(r_t, r_2)$. $B_A(L, \phi, r_t)$ has already been determined (Equation 19). Rewriting Equation 9, we have:

$$dI(\theta) = \sigma(\theta)\, E(\ell)\, dV \qquad 25$$

where:

$dI(\theta)$ = the intensity of backscattered light from a small volume of water dV along the line of sight. (Units = watts/steradian-nanometer)

$\sigma(\theta)$ = the volume-scattering function. (Units = 1/meter-steradian)

$E(\ell)$ = the irradiance at a distance ℓ from the source. (Units = watts/meter^2-nanometer)

dV = dAdr = element of volume along the line of sight with length dr and area dA normal to the line of sight. (Units = meter^3)

θ = backscattering angle as defined in Figure 14.

The radiance of this backscattering element dV at the location of the underwater camera (due to light of wavelength λ) is approximately:

$$dE_B(r) = \frac{dI(\theta)}{dA} e^{-\alpha r}$$

$$= \sigma(\theta)\, E(\ell) e^{-\alpha r}\, dr$$

$$\text{or} \quad dE_B(r) = \frac{I\sigma(\theta) e^{-\alpha r}}{\ell^2} (e^{-\alpha \ell} + c_1 K \ell e^{-K\ell} + C_2 K \ell e^{-2K\ell})\, dr \qquad 26$$

where $r = \ell \cos \theta$

In most cases the underwater light source will be located relatively close to the camera, and distances ℓ and r can be assumed to be approximately equal. If we further assume that the illumination is uniform across the light beam and that the volume-scattering function $\sigma(\theta)$ is independent of angle θ in the backscattering region, then Equation 26 can be integrated as follows:

$$E_B(r_1,r_2) \approx \sigma I \left[\int_{r_1}^{r_2} \frac{e^{-2\alpha r}}{r^2}\, dr + C_1 K \int_{r_1}^{r_2} \frac{e^{-(\alpha+K)r}}{r}\, dr + C_2 K \int_{r_1}^{r_2} \frac{e^{-(\alpha+2K)r}}{r}\, dr \right] \qquad 27$$

where: $E_B(r_1,r_2)$ = the radiance of the line of sight from r_1 to r_2 at the location of the camera due to backscattering of light at wavelength λ (units = watts/steradian-meter^2 - nanometer).

The total luminance of the line of sight from r_1 to r_2 at the location of the camera can be calculated as follows:

$$B_B(r_1,r_2) = \int_{400nm}^{700nm} E_B(r_1,r_2)\, L(\lambda)\, d\lambda \qquad 28$$

where $B_B(r_1,r_2)$ and $L(\lambda)$ are as previously defined. $B_B(r_1,r_2)$ can be calculated from Equations 27 and 28 if the limits of integration are revised (1).

A computer program has been written to solve Equations 18, 19 and 24 using numerical techniques. In addition, the program is capable of computing the luminous efficiency of a lighting system. Appendix II presents this program and discusses its use.

IV. DESIGN ANALYSIS OF TYPICAL UNDERWATER LIGHTING SYSTEMS

Section III developed several expressions which may be used to analyze the design of an underwater lighting system. While these expressions could be solved by hand, they are more readily solved using a digital computer. The following examples serve to illustrate the use of Equations 18, 19 and 24 in design analysis, and the use of the digital computer in solving these equations.

Example 1: Problem

Figure 15 illustrates a proposed design of a deep sea photographic system to be used for bottom photography. Assuming clear ocean water and a clay bottom, determine the optimum camera-lamp spacing. If the light source is to be a 1000 watt incandescent lamp mounted in a reflecting enclosure, what is the spectral distribution of the reflected light received by the camera? If the camera has a f4.5 lens, what is the correct shutter speed for ASA250 film? What is the luminous efficiency of the light source?

Example 1: Solution

Step 1: Determine A(N) and K(N).

Values for the attenuation and diffuse attenuation coefficients, A(N) and K(N), were obtained from Reference 23 at each 10 nanometer increment between 400 and 700 nanometers wavelength.

Step 2: Determine SIGMA.

Since backscattering in clear ocean water is approximately two or three times that predicted by the Rayleigh Theory (Equation 11), SIGMA was set at $3\sigma_R(180°)$. (1)

Figure 15

Deep Sea Photographic System

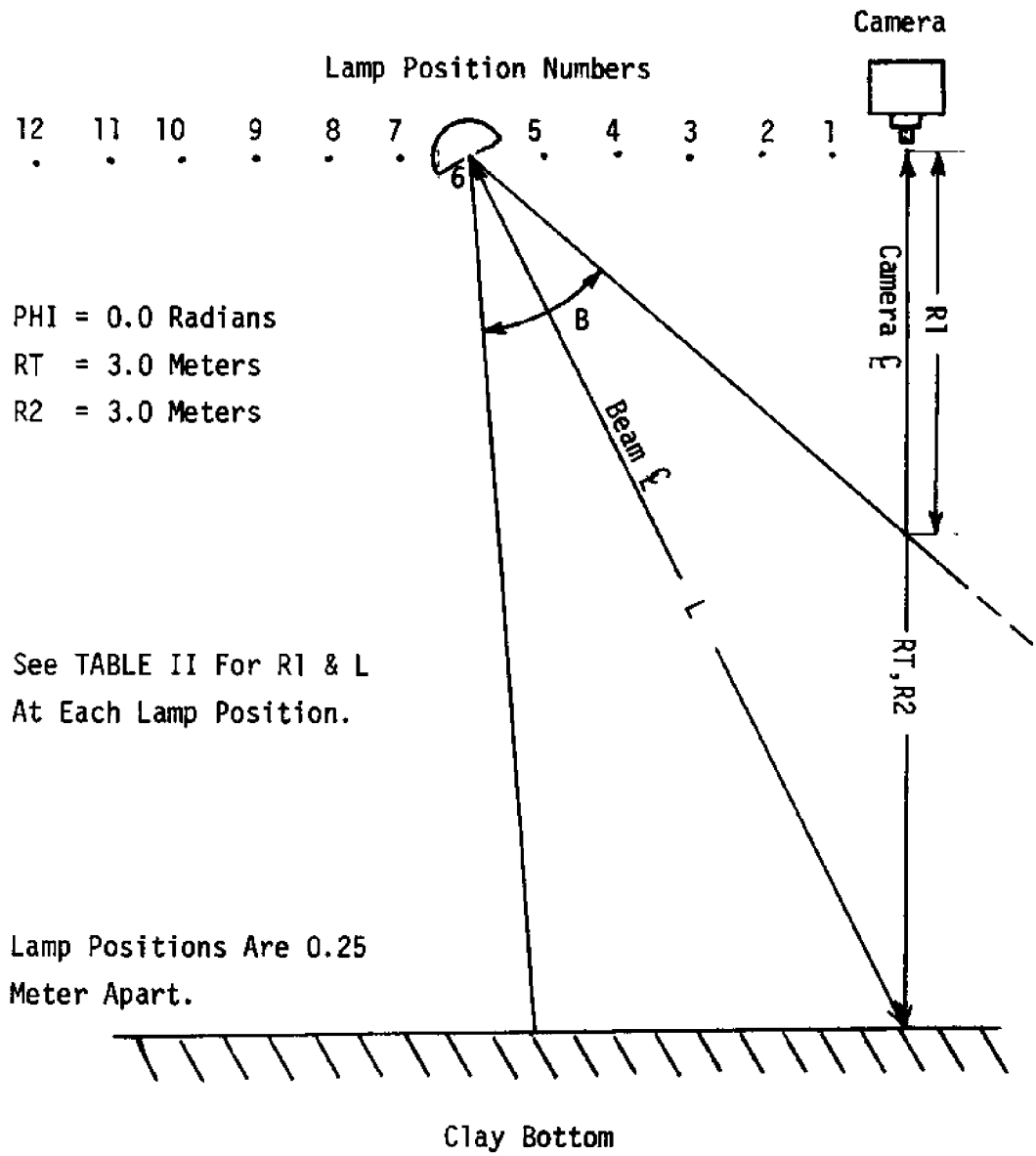

Step 3: Determine C3.

The diffuse reflectivity coefficients of various materials are listed in Reference 24. C3 was determined to be 0.82.

Step 4: Determine PHI and RT.

PHI and RT were evaluated by inspection of Figure 15. PHI = 0.0 radians and RT = 3.00 meters.

Step 5: Determine LE(N).

For this analysis, the standard relative luminosity curve was assumed applicable. Under this assumption, the appropriate lumens/watt conversion factors were obtained from Reference 4 at each 10 nanometer increment between 400 and 700 nanometers wavelength.

Step 6: Determine NL.

The number of lamps, NL, was determined from the problem statement. NL=1.

Step 7: Determine I(N) for each lamp.

The problem stated that a 1000 watt incandescent lamp would be used. Assuming the lamp converts electrical watts to radiant watts with an efficiency of 11.5% (typical), and assuming the lamp is mounted in a reflector having an efficiency of 50% (also typical), then we can calculate the radiant power contained in the lamp beam:

Lamp power	X	Lamp Efficiency	X	Reflector Efficiency	=	Radiant Beam Power
1000 watts	X	11.5%	X	50%	=	57.5 watts.

If this power is concentrated in a uniform beam $\pi/4$ radians wide, then the radiant intensity of the lamp is 73.2 watts/steradian. Since most incandescent lamps used in underwater applications approximate a 3400°K blackbody source, we can assume a straight line approximation for lamp intensity I_λ (watts/steradian-nanometer), with:

$$I_{400nm} \simeq 0.18\ I_{700nm},$$

and:

Total Radiant Intensity = $\int_{400nm}^{700nm} I_\lambda \, d\lambda$ = 73.2 watts/steradian.

Under these assumptions, I(N) was easily evaluated at each 10 nanometer increment between 400 and 700 nanometers wavelength. (1, 19)

Step 8: Determine WT for each lamp.

The total electrical power drawn by the lamp was given in the problem statement as 1000 watts.

Step 9: Determine B and RE for each lamp.

The beam width of the lamp was assumed to be $\pi/4$ radians. Reflector efficiency was assumed to be 50%.

Step 10: Determine R1, R2, and L for each lamp.

To determine the optimum camera-lamp spacing, it was decided that the computer program should be run at twelve different lamp positions, as indicated in Figure 15. At each position, the light beam was assumed to be centered on the clay bottom directly beneath the camera. Thus, R1 and L were easily determined using trigonometry, and R2 was set equal to RT for the entire problem.

Having completed Step 10, we then had all the required data for input into the computer. The program was run at each of the twelve lamp positions, and the results are summarized in Table II and Figure 16.

Based on this analysis, position 6 was identified as the optimum location for the lamp. This position yields the highest subject contrast, and will produce photographs with minimum interference from backscattering. The subject luminance and spectral radiance at this position are also satisfactory.

Because of non-uniformity of the spectral radiance received by the camera (Figure 16), spectral filtering will be required for satisfactory color photography, regardless of lamp position. Several color correction filters are

TABLE II

Contrast, Subject Luminance and Lamp Luminous Efficiency for Example 1.

POSITION	L (METERS)	R1 (METERS)	CONTRAST	SUBJECT LUMINANCE (LUMENS/SR-M^2)
1	3.010	0.485	7.6	308.6
2	3.041	0.801	15.2	301.6
3	3.092	1.012	21.4	290.7
4	3.162	1.153	25.5	276.5
5	3.250	1.245	27.8	260.0
6	3.354	1.301	28.5	242.2
7	3.473	1.330	27.3	223.8
8	3.606	1.339	25.4	205.4
9	3.750	1.332	23.0	187.7
10	3.905	1.312	20.4	170.9
11	4.070	1.282	17.4	155.2
12	4.243	1.243	15.0	140.7

Luminous efficiency of the lamp = 29.5 LUMENS/WATT
Increment size used = 0.1 METER

Figure 16

Spectral Radiance for Example 1

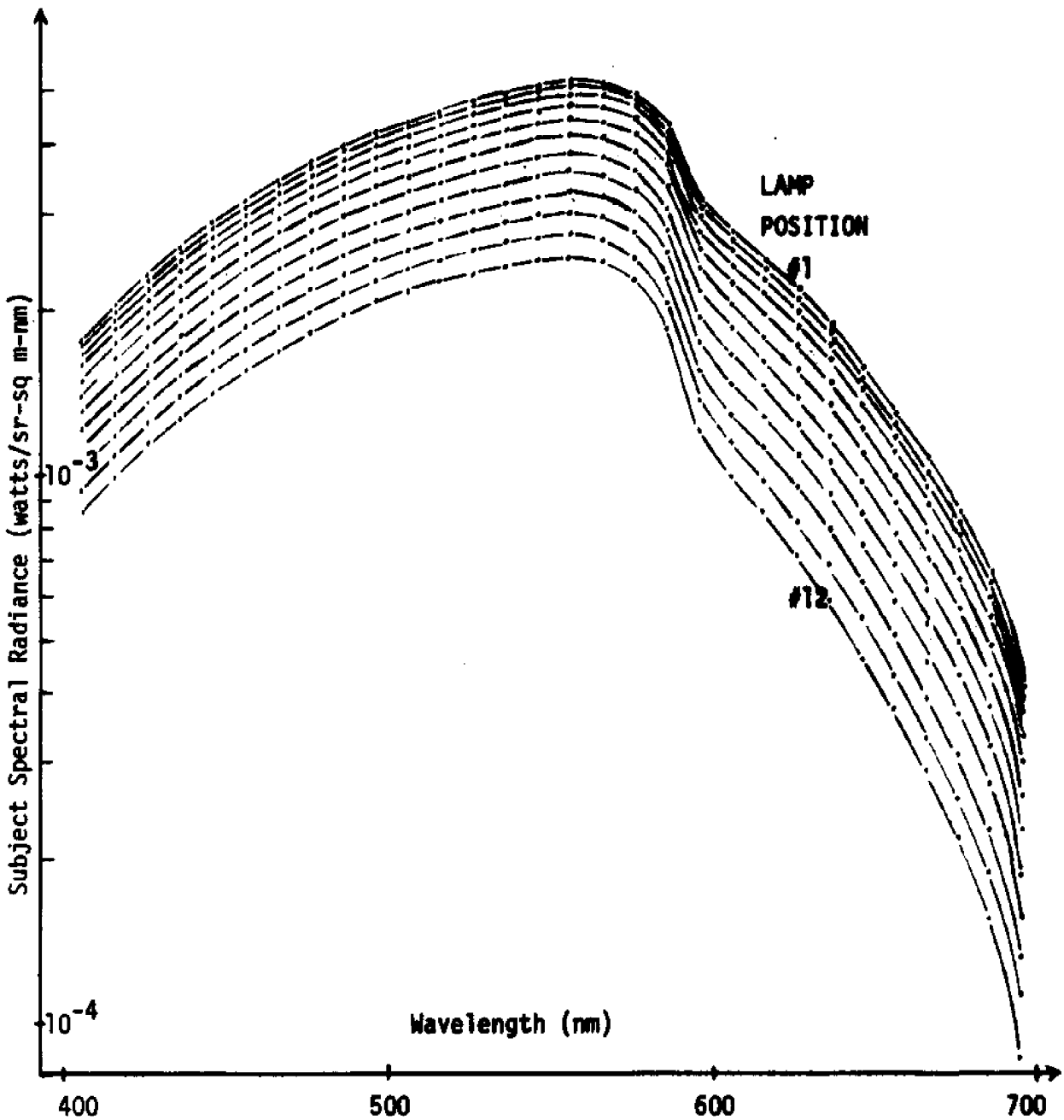

commercially available which would be effective for the short path lengths involved in this design. However, use of a filter requires an adjustment in camera f-stop, shutter speed, or both. For the purpose of this example, a CC40M filter is used to produce a nearly uniform spectral radiance distribution at the lens and a 1.5 f-stop loss in effective camera aperture.

Correct shutter speed can be calculated from Equation 20. Rearranging and substituting known quantities, we have for position 6:

$$t = \frac{Kf^2}{(ASA)B}$$

$$t = \frac{(12.65)(4.5 + 1.5)^2}{(250)\ (242.2)}$$

$$t = 0.0075 \text{ seconds} \sim 1/125 \text{ seconds}$$

Luminous efficiency of the lamp was calculated to be 29.5 lumens/watt, which is reasonable for an underwater incandescent bulb. Luminous efficiencies approaching 35 lumens/watt are attainable in gas-filled incandescent bulbs designed for underwater use, while simple 25 watt household incandescent bulbs can have luminous efficiencies as low as 10 lumens/watt. (1)

Example 2: Problem

A deep submergence submarine was constructed with a viewing area geometry as illustrated in Figure 17. The viewing area was illuminated by four 500 watt incandescent lamps and two 250 watt thallium iodide-mercury vapor lamps. During sea trials, color photographs taken from the viewports were noted to lack proper color balance. The shipyard engineer recommended replacement of the thallium iodide - mercury vapor lamps with dysprosium - thallium iodide lamps of the same power rating. Was this recommendation reasonable?

Four 250 watt thallium iodide-mercury vapor lamps are mounted on the

Figure 17

Deep Submergence Submarine Viewing Area

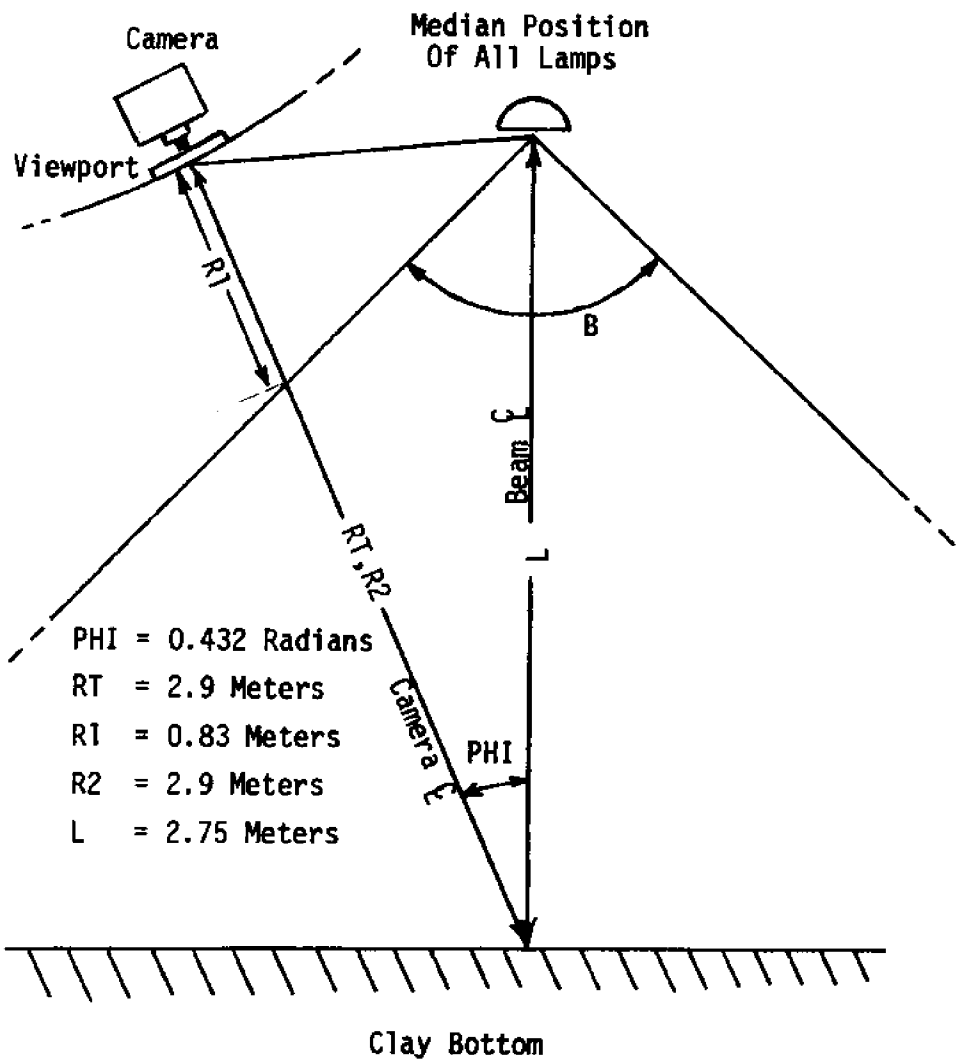

bow of the submarine to provide illumination for a forward looking search and obstacle avoidance black-and-white television system. Would this illumination be improved by substituting dysprosium-thallium-iodide lamps for the thallium iodide-mercury vapor lamps? For the purpose this second question, assume there is a clay bank (obstacle) directly in front of the submarine at a range of approximately eight meters. The following dimensions are provided for each lamp:

PHI = 0.0 radians
RT = 8.0 meters
R1 = 1.82 meters
R2 = 8.0 meters
L = 7.7 meters

Example 2: Solution

Question A

Steps 1, 2, and 3: Determine A(N), K(N), SIGMA, and C3.

The values used for Example 1 were assumed applicable.

Step 4: Determine PHI and RT.

PHI and RT were evaluated by inspection of Figure 17. PHI = 0.432 radians and RT = 2.9 meters.

Step 5: Determine LE(N).

The values used for Example 1 were assumed applicable.

Step 6: Determine NL .

For reasons to be discussed in Step 7, the number of lamps, NL, was set at two (2).

Step 7: Determine I(N) for each lamp.

The problem stated that four 500 watt incandescent lamps and two 250 watt thallium iodide-mercury vapor lamps were installed. Since these lamps are close together and symmetrically mounted, the lamp-to-subject

distance, L, is nearly identical for each lamp, and we can analyze the problem as if a single 2000 watt incandescent lamp and a single 500 watt thallium iodide-mercury vapor lamp were each mounted at the median position. This reduces the length of the computer run and reduces the cost.

Assuming the (composite) 2000 watt incandescent lamp has a radiant efficiency of 11.5% and a reflector efficiency of 50%, then the radiant power contained in the lamp beam is 115 watts. If this power is concentrated in a uniform beam $\pi/2$ radians wide, then the radiant intensity is 73.2 watts/steradian, which is the same intensity as the lamp of Example 1. Thus, we can re-use the I(N) values assigned in the previous example.

Analysis of the (composite) 500 watt thallium iodide-mercury vapor lamp is accomplished in a similar manner. Assuming the arc lamp converts electrical watts to radiant watts with an efficiency of 22.1% (typical), and assuming the reflector efficiency and beam width are the same as for the incandescent lamp, then the radiant intensity is 35.2 watts/steradian. Since nearly 70% of the visible emission of a thallium iodide-mercury vapor lamp is contained in the region 530-550 nanometers wavelength, with the remainder of the energy distributed more or less uniformly over the rest of the visible spectrum, I(N) values can be easily assigned. As before,

$$\int_{400nm}^{700nm} I(N)\, d\lambda$$

must equal the total radiant intensity.

Analysis of the (composite) 500 watt dysprosium-thallium-iodide lamp is identical with that of the thallium iodide-mercury vapor lamp, except for assignment of I(N) values. These are determined from the spectral distribution curve (Figure 18) and the radiant intensity. (1, 19, 21)

Step 8: Determine WT for each lamp.

The total electrical power drawn by the composite incandescent lamp is 2000 watts. The composite thallium iodide-mercury vapor and dysprosium-thallium-iodide lamps each draw 500 watts.

Step 9: Determine B and RE for each lamp.

The beam width of each lamp was assumed to be $\pi/2$ radians. Reflector efficiency was assumed to be 50%.

Step 10: Determine R1, R2, and L for each lamp.

R1, R2, and L were determined by evaluation of Figure 17. R1 = 0.83 meters, R2 = 2.9 meters and L = 2.75 meters.

To evaluate the effect of replacing the thallium iodide-mercury vapor lamps with dysprosium-thallium-iodide lamps, the computer program had to be run twice, once for each situation. The results are summarized in Table III and Figure 19.

Based on this analysis, the shipyard engineer's recommendation was reasonable. The dysprosium-thallium-iodide lamps (in conjunction with the incandescent lamps) provide more light energy in the red and violet regions of the visible spectrum than the thallium iodide-mercury vapor lamps. The resulting spectrum is more uniform and is easily correctable with CC30M filter (or equivalent). The spectrum provided by the thallium iodide-mercury vapor lamps (in conjunction with the incandescent lamps) has an extremely strong peak near 535nm. This peak will produce a greenish cast to any color photograph, and is not easily correctable by

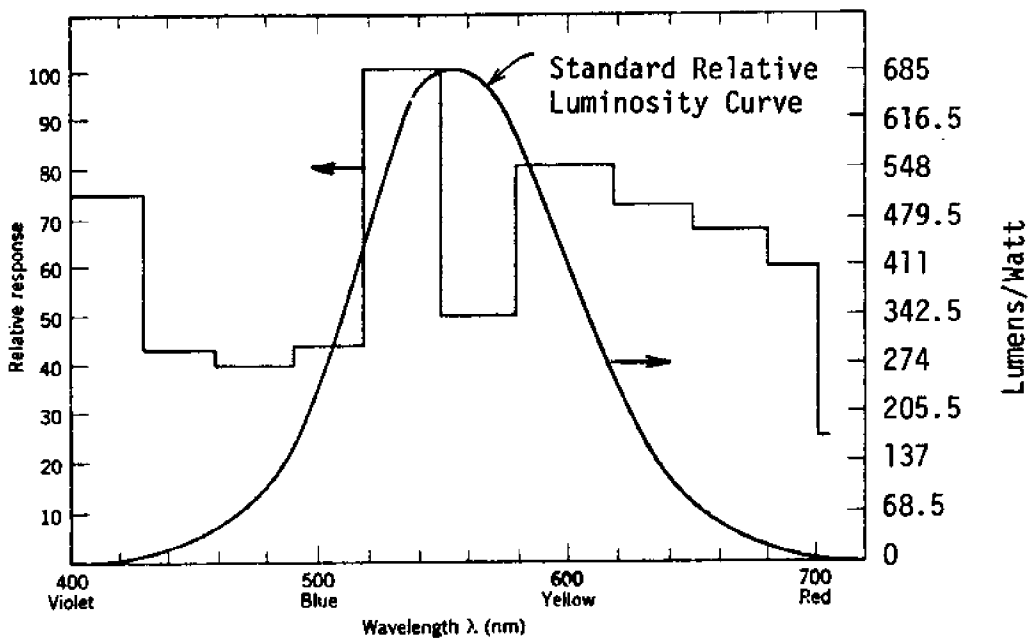

Figure 18. Spectral output of a dysprosium-thallium iodide lamp. (1)

TABLE III

Composite Contrast, Luminance, and Lamp Luminous Efficiency for Example 2A

	CONTRAST	LUMINANCE (LUMENS/SR-M^2)	LUMINOUS EFFICIENCY (LUMENS/WATT)
INCANDESCENT + THALLIUM IODIDE LAMPS	20.0	718.0	43.7
INCANDESCENT + DYSPROSIUM-THALLIUM IODIDE LAMPS	19.0	531.3	35.5

Luminous efficiency of incandescent source = 29.5 LUMENS/WATT
Luminous efficiency of TI source = 100.6 LUMENS/WATT
Luminous efficiency of DTI source = 59.4 LUMENS/WATT
Increment size used = 0.05 METER

Figure 19

Spectral Radiance for Example 2A

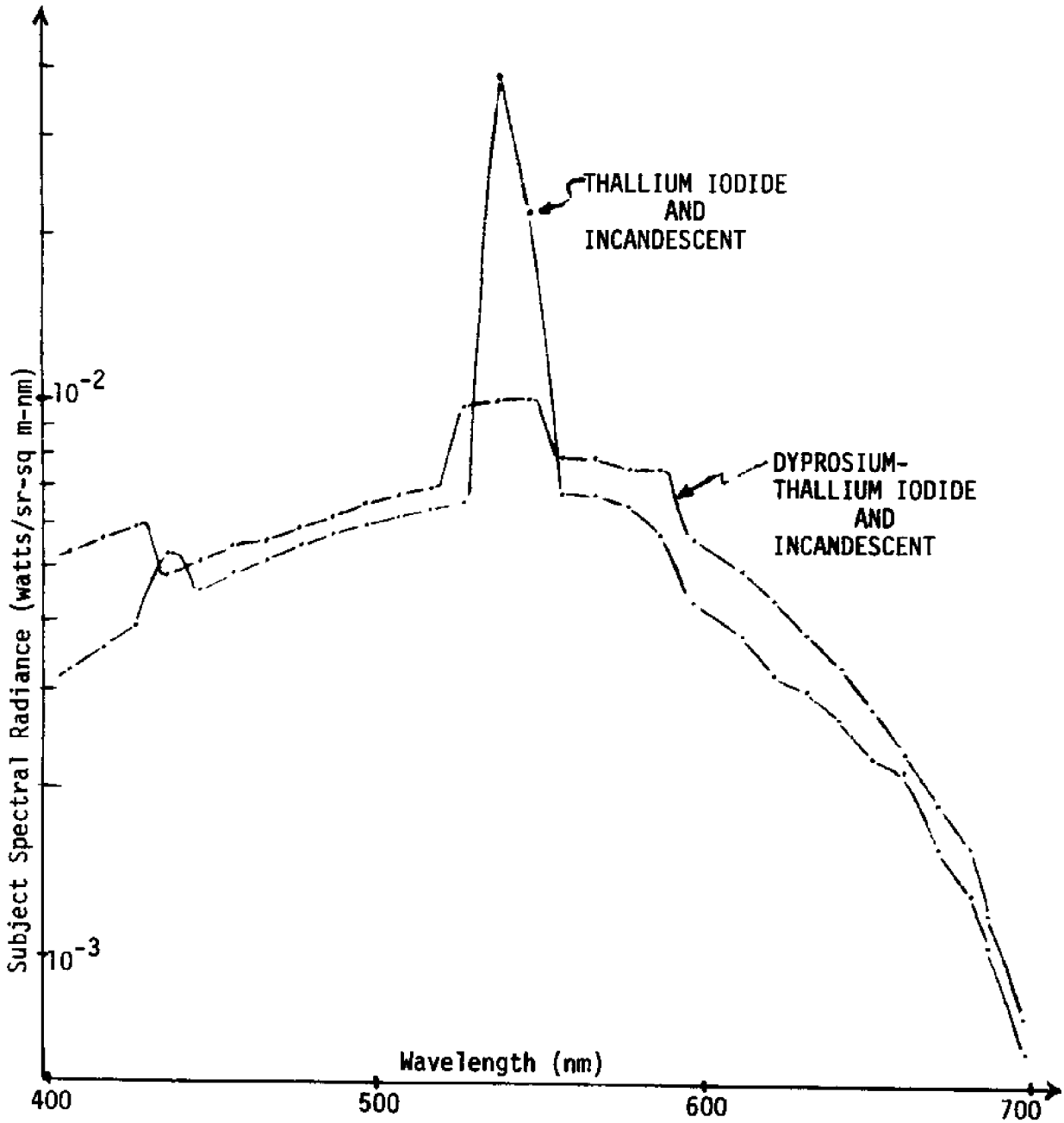

filtering. On the other hand, the differences in subject contrast and luminance are relatively minor and can be ignored for the purposes of this comparison.

Question B

The same data used in Question A was used to solve Question B, except as noted:

Step 4: Determine PHI and RT.

PHI and RT were given in the problem statement as 0.0 radians and 8.0 meters, respectively.

Step 5: Determine LE(N).

The sensitivity of a typical black-and-white television vidicon as a function of wavelength was obtained from Reference 19 at each 10 nanometer increment between 400 and 700 nanometers wavelength. The units of LE(N) for this analysis are vidicon amperes/radiant watt.

Step 6: Determine NL.

For reasons to be discussed in Step 7, the number of lamps, NL, was set at two (2).

Step 7: Determine I(N) for each lamp.

The problem stated that either four 250 watt thallium iodide-mercury vapor lamps or four 250 watt dysprosium-thallium-iodide lamps would be used for forward-looking television illumination. Since these lamps are close together and symmetrically mounted, the lamp-to-subject distance, L, is nearly the same for each lamp, and we can analyze the problem as if two 500 watt arc lamps were located at the median position. Thus we can use the I(N) values assigned in Question A.

Step 8: Determine WT for each lamp.

The total electrical power drawn by each composite lamp is 500 watts.

Step 9: Determine B and RE for each lamp.

The beam width of each lamp was assumed to be $\pi/2$ radians. Reflector efficiency was assumed to be 50%.

Step 10: Determine R1, R2, and L for each lamp.

R1, R2, and L were given in the problem statement as 1.82, 8.0, and 7.7 meters, respectively.

The program was run for two cases: first, with thallium iodide-mercury vapor lamps installed, and second, with dysprosium-thallium-iodide lamps installed. The results are summarized in Table IV.

Based on this analysis, the thallium iodide-mercury vapor lamps should be retained for forward-looking black-and-white television illumination. These lamps produce greater subject contrast and nearly twice the luminance of the dysprosium-thallium iodide arc lamps.

TABLE IV

Composite Contrast and Luminance for Example 2B

	CONTRAST	LUMINANCE (VIDICON AMPERES/SR-M^2)
THALLIUM IODIDE LAMPS	3.56	0.0090
DYSPROSIUM-THALLIUM IODIDE LAMPS	3.23	0.0055

Increment size used = 0.05 METER

APPENDIX I. - BIBLIOGRAPHY

(1) Mertens, Lawrence E., In-Water Photography, Theory and Practice, New York: Wiley-Interscience, 1970.

(2) Duntley, Siebert Q., "Light in the Sea", Journal of the Optical Society of America, 53, 214-233 (1963).

(3) Jerlov, N. G., Optical Oceanography, New York: American Elsevier, 1968.

(4) Kingslake, Rudolf, Applied Optics and Optical Engineering, New York: Academic Press (1965).

(5) Hulbert, E.O., "Optics of Distilled and Natural Water," Journal of the Optical Society of America, 35, 698-705 (1945).

(6) Neumann, Gerhard and Pierson, Willard J., Jr., Principles of Physical Oceanography, Englewood Cliffs, N.J.: Prentice-Hall, 1966.

(7) Hill, M. N, ed., The Sea, Vol. I, New York: Wiley-Interscience, 1962.

(8) Sverdrup, H. U., Johnson, Martin W., and Fleming, Richard H., The Oceans, Englewood Cliffs, N. J.: Prentice-Hall, 1942.

(9) Duntley, Siebert Q., "Visibility in the Oceans", Optical Spectra, Fourth Quarter, 1967, 64-69.

(10) Curcio, Joseph A., and Petty, Charles C., "The Near Infrared Absorption Spectrum of Liquid Water", Journal of the Optical Society of America, 41, 302-304 (1951).

(11) Dawson, L. H. and Hulbert, E. O., "The Absorption of Ultraviolet and Visible Light by Water", Journal of the Optical Society of America, 24, 175-177 (1934).

(12) Sullivan, Seraphin A., "Experimental Study of the Absorption in the Distilled Water, Artifical Sea Water, and Heavy Water in the Visible Region of the Spectrum," Journal of the Optical Society of America 53, 962-968 (1963).

(13) Sinclair, David, "Light Scattering by Spherical Particles", Journal of the Optical Society of America, 37, 475-480 (1947).

(14) Morel, A., "Optical Properties of Pure Water and Pure Sea Water", in Optical Aspects of Oceanography, edited by N. G. Jerlov and E. Steelmann Nielsen, New York: Academic Press, 1974.

(15) Dawson, L. H. and Hulbert, E. O., "Angular Distribution of Light Scattered in Liquids", Journal of the Optical Society of America, 31, 554-558 (1941).

(16) Kullenberg, G., "Observed and Computed Scattering Functions", in Optical Aspects of Oceanography, Edited by N. G. Jerlov and E. Steelmann Nielsen, New York: Academic Press, 1974.

(17) Woodard, David W., "Multiple Light Scattering by Spherical Dielectric Particles", Journal of the Optical Society of America, 54, 1325-1331 (1964).

(18) Hersey, John Brackett, ed., Deep-Sea Photography, Baltimore: Johns Hopkins Press (1967).

(19) Naval Undersea Center, NUCTP 303. Handbook of Underwater Imaging System Design, by C. J. Funk, S. B. Bryant, and P. J. Heckman, Jr., San Diego, California, July 1972.

(20) Reiling, Gilbert H., "Characteristics of Mercury Vapor-Metallic Iodide Arc Lamps", Journal of the Optical Society of America, 54, 532-540 (1964).

(21) Larson, D. A. and Rixton, F. H., "Underwater Lighting and New Light Sources", Undersea Technology, September 1969, 38.

(22) Duntley, Siebert Q., Boileau, A. R., and Preisendorfer, R. W., "Image Transmission by the Troposphere," Journal of the Optical Society of America, 47, 499-506 (1957).

(23) Tyler, John E., Smith, Raymond C., and Wilson, Wayne H., Jr., Predicted Optical Properties for Clear Natural Water", Journal of the Optical Society of America, 62, 83-91 (1972).

(24) Weast, Robert C., ed., Handbook of Chemistry and Physics, Cleveland: CRC Press, 1974.

APPENDIX II. - COMPUTER PROGRAM

This appendix presents a computer program which can be used to analyze any underwater lighting system. The following data must be provided as an input to the computer:

D		The increment size into which distance R_1 to R_2 is to be subdivided for purposes of numerical integration. (Units = meters)
A(N)	N = 1, 2,..., 30	Values for the attenuation coefficient at each 10 nanometer increment between 400 and 700 nanometers wavelength. (Units = $meter^{-1}$)
K(N)	N = 1, 2,..., 30	Values for the diffuse attenuation coefficient at each 10 nanometer increment between 400 and 700 nanometers wavelength. (Units = $meter^{-1}$)
SIGMA		The value of the volume scattering function for all backscattering directions. (Units = 1/meter-steradian)
C3		The reflectivity of the diffuse subject being photographed. $0 < C3 \leq 1$. (Units = dimensionless)
PHI		The viewing angle of the subject, measured relative to the surface normal. (Units = radians)
RT		The distance from the camera to the subject. (Units = meters)
LE(N)	N = 1, 2,..., 30	The sensitivity of the receiver at each 10 nanometer increment between 400 and 700 nanometers wavelength. The standard relative luminosity curve should be used for most applications. (Units = lumens/watt)
NL		The number of lamps being included in the analysis.

For each lamp, the following data must be provided:

I(N) N = 1, 2,..., 30	Values for the lamp intensity at each 10 nanometer increment between 400 and 700 nanometers wavelength. (Units = watts/steradian-nanometer)
WT	The total electrical power drawn by the lamp. (Units = watts)
B	The beam width of the lamp. (Units = radians)
RE	The efficiency of the reflector. $0 \leq RE \leq 1$. (Units = dimensionless)
R1	The distance from the camera to the closest point along the line of sight that is illuminated by the lamp. (Units = meters)
R_2	The distance from the camera to the farthest point along the line of sight that is illuminated by the lamp. (Units = meters).
L	The distance from the lamp to the subject. (Units = meters)

The following information will be available as an output from the computer:

EB(N) N = 1, 2,..., 30 (for each lamp)	Values for the subject radiance at the location of the camera at each 10 nanometer increment between 400 and 700 nanometers wavelength. (Units = watts/steradian-square meter-nanometer)
BBT (for each lamp)	Subject luminance at the location of the camera due to the lamp. (Units = lumens/steradian-square meter)
LEL (for each lamp)	Luminous efficiency of the lamp. (Units = lumens/watt)

C (for each lamp)	Contrast of the subject due to the lamp. (Units = dimensionless)
TEB(N) N = 1, 2,..., 30	Values for the subject radiance at the location of the camera at each 10 nanometer increment betwen 400 and 700 nanometers wavelength due to all lamps. (Units = watts/ steradian-square meter-nanometer)
TBBT	Subject luminance at the location of the camera due to all lamps. (Units = lumens/steradian-square meter)
TLEL	Composite luminous efficiency of all lamps. (Units = lumens/watt)
TC	Contrast of the subject due to all lamps. (Units = dimensionless)

Figure 20 is a flow chart of the computer program.

Figure 20

Flow Chart of Computer Program

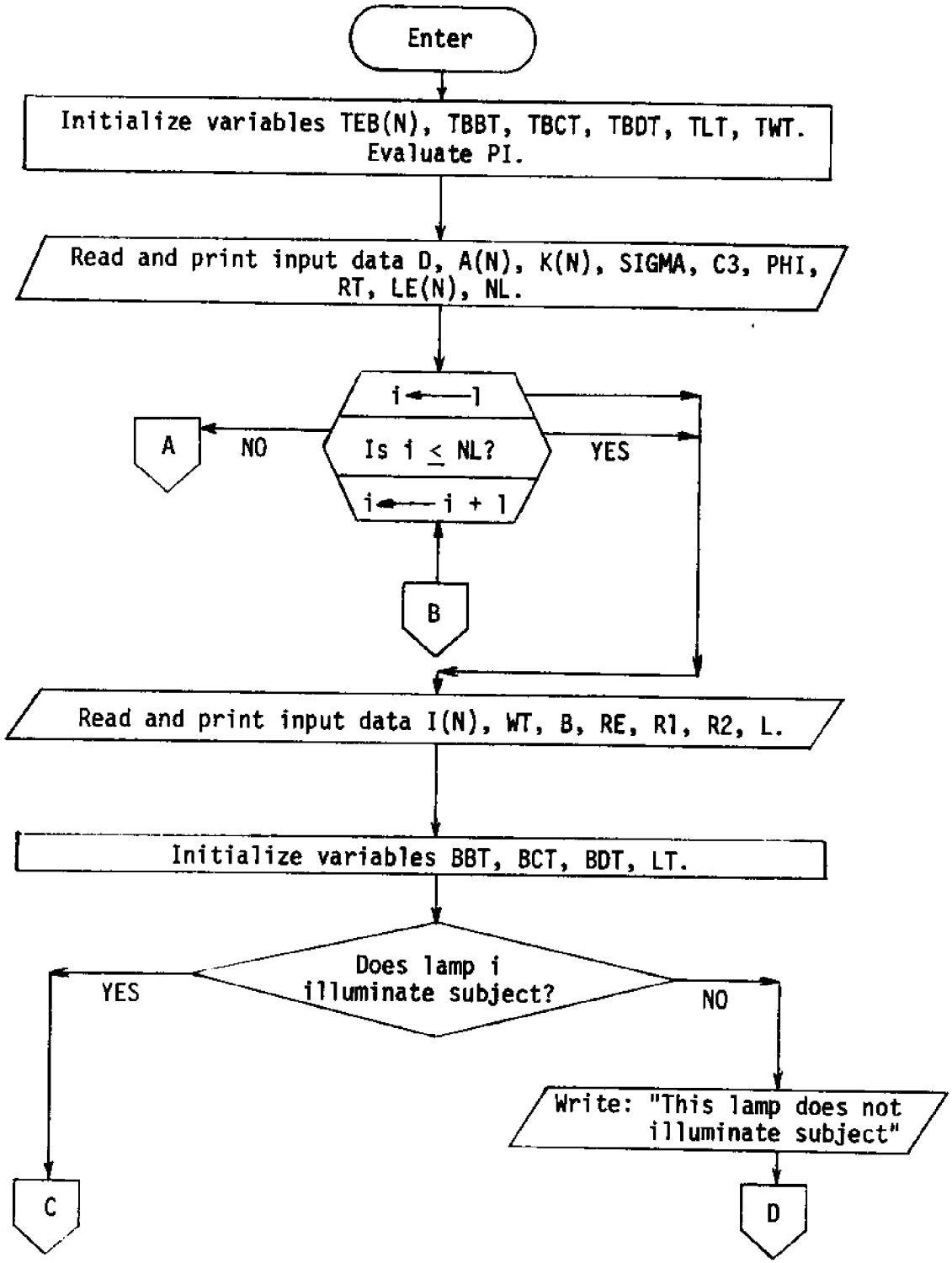

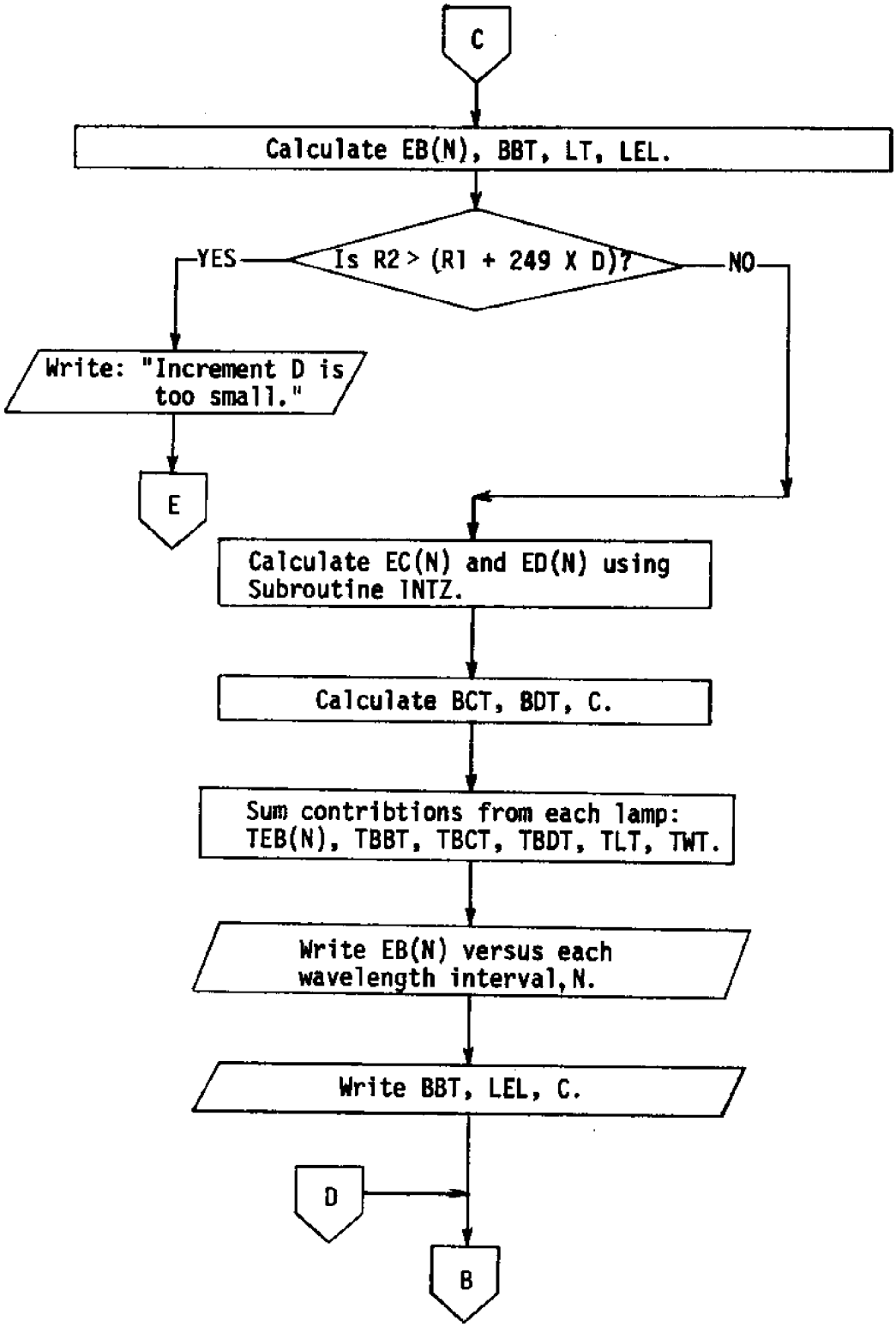
C
Calculate EB(N), BBT, LT, LEL.
Is R2 > (R1 + 249 X D)?
YES
NO
Write: "Increment D is too small."
E
Calculate EC(N) and ED(N) using Subroutine INTZ.
Calculate BCT, BDT, C.
Sum contribtions from each lamp: TEB(N), TBBT, TBCT, TBDT, TLT, TWT.
Write EB(N) versus each wavelength interval, N.
Write BBT, LEL, C.
D
B

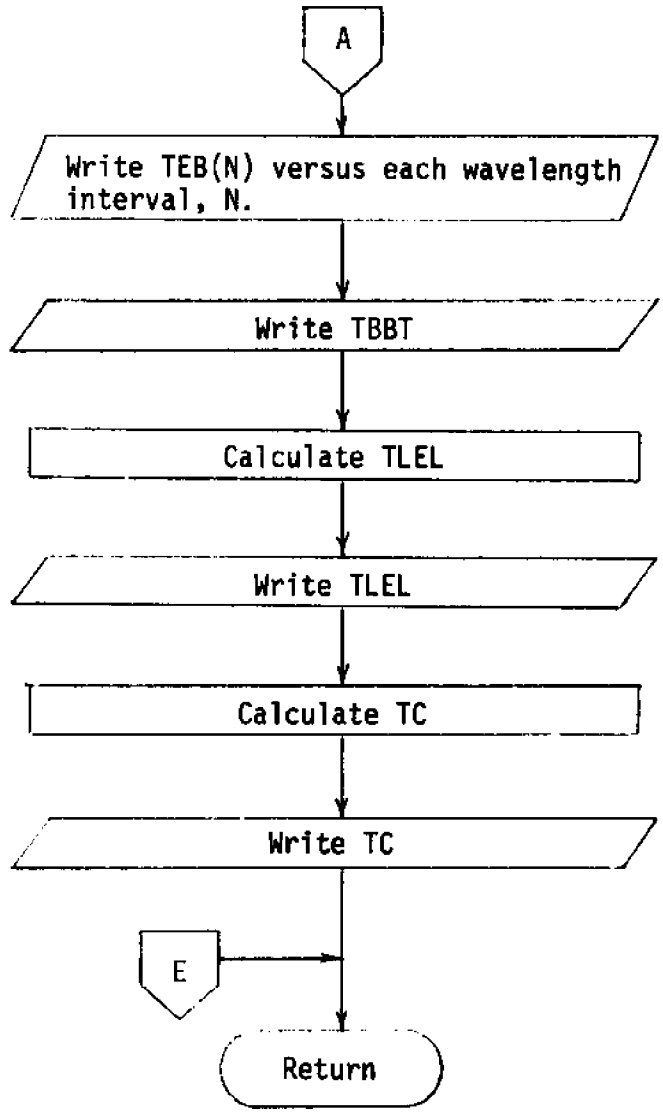

Subroutine INTZ

This subroutine performs numerical integration using the trapezoidal rule.

```
   //JOB
   //*PASSWORD
   //*WATFIV
   C PROGRAMMER: B. D. GREESON
   C COURSE: CE-685
   C NATURE OF PROBLEM: ANALYZE A PROPOSED DESIGN FOR A SUPPLEMENTAL
   C LIGHTING SYSTEM TO BE USED IN UNDERWATER PHOTOGRAPHY.
   C METHOD OF SOLUTION: NUMERICAL SOLUTION OF IMPORTANT EQUATIONS
   C DEVELOPED IN SECTION III.  FOR ADDITIONAL INFORMATION REGARDING
   C THIS COMPUTER PROGRAM, SEE SECTION IV.
 1       REAL A(30)
   C ARRAY A CONTAINS VALUES FOR THE ATTENUATION COEFFICIENT AT EACH
   C TEN (10) NANOMETER INCREMENT BETWEEN 400 AND 700 NANOMETERS
   C WAVELENGTH (1/METER).
 2       REAL B
   C VARIABLE B IS THE BEAM WIDTH OF THE LAMP (RADIANS, STERADIANS).
 3       REAL BBT
   C VARIABLE BBT IS THE SUBJECT LUMINANCE AT THE LOCATION OF THE
   C CAMERA DUE TO THE LAMP (LUMENS/STERADIAN-SQ METER).
 4       REAL BCT
   C VARIABLE BCT IS THE LUMINANCE OF THE LINE OF SIGHT BETWEEN  R1
   C AND R2 DUE TO THE LAMP (LUMENS/STERADIAN-SQ METER).
 5       REAL BDT
   C VARIABLE BDT IS THE LUMINANCE OF THE LINE OF SIGHT BETWEEN RT
   C AND R2 DUE TO THE LAMP (LUMENS/STERADIAN-SQ METER).
 6       REAL C
   C VARIABLE C IS THE CONTRAST OF THE SUBJECT DUE TO THE LAMP
   C (DIMENSIONLESS).
 7       REAL C1, C2
   C VARIABLES C1 AND C2 ARE CALCULATED CONSTANTS USED IN THE ANALYSIS.
 8       REAL C3
   C VARIABLE C3 IS THE REFLECTIVITY OF A DIFFUSE SUBJECT (0-1,
   C DIMENSIONLESS).
 9       REAL D
   C VARIABLE D IS THE INCREMENT SIZE INTO WHICH THE DISTANCE R1 TO
   C R2 IS SUBDIVIDED FOR INSERTION INTO THE X ARRAY.  D CAN BE SELECTED
   C ARBITRARILY, PROVIDED D IS NO SMALLER THAN (R2-R1)/249 (METERS).
10       REAL EA(30)
   C ARRAY EA CONTAINS VALUES FOR THE IRRADIANCE OF THE SUBJECT BY THE
   C LAMP AT EACH WAVELENGTH INTERVAL (WATTS/SQ METER-NANOMETER).
11       REAL EB(30)
   C ARRAY EB CONTAINS VALUES FOR THE SUBJECT RADIANCE AT THE LOCATION
   C OF THE CAMERA AT EACH WAVELENGTH INTERVAL DUE TO THE LAMP (WATTS/
   C STERADIAN-SQ METER-NANOMETER).
12       REAL EC(30)
   C ARRAY EC CONTAINS VALUES FOR THE RADIANCE OF THE LINE OF SIGHT
```

```
C BETWEEN R1 AND R2 AT EACH WAVELENGTH INTERVAL DUE TO THE LAMP
C (WATTS/STERADIAN-SQ METER-NANOMETER).
13      REAL ED(30)
C ARRAY ED CONTAINS VALUES FOR THE RADIANCE OF THE LINE OF SIGHT
C BETWEEN RT AND R2 AT EACH WAVELENGTH INTERVAL DUE TO THE LAMP
C (WATTS/STERADIAN-SQ METER-NANOMETER).
14      REAL FX1(30,250), FX2(30,250), FX3(30,250)
C ARRAYS FX1, FX2, AND FX3 ARE FUNCTION VALUES USED IN THE CALCU-
C LATION OF SUBJECT CONTRAST.
15      REAL I(30)
C ARRAY I CONTAINS VALUES FOR THE LAMP INTENSITY AT EACH WAVELENGTH
C INTERVAL (WATTS/STERADIAN-NANOMETER).
16      REAL INT1(30), INT2(30), INT3(30), INT4(30), INT5(30), INT6(30)
C ARRAYS INT1, INT2, INT3, INT4, INT5, AND INT6 ARE DEFINITE
C INTEGRALS OF FUNCTION VALUES FX1, FX2, AND FX3, AND ARE USED IN
C THE CALCULATION OF SUBJECT CONTRAST.
17      INTEGER J
C VARIABLE J IS A COUNTER USED IN THE MASTER (OUTERMOST) DO-LOOP.
18      REAL K(30)
C ARRAY K CONTAINS VALUES FOR THE DIFFUSE ATTENUATION COEFFICIENT
C AT EACH WAVELENGTH INTERVAL (1/METER).
19      REAL L
C VARIABLE L IS THE DISTANCE FROM THE LAMP TO THE SUBJECT (METERS).
20      REAL LE(30)
C ARRAY LE CONTAINS VALUES FOR THE SENSITIVITY OF THE RECEIVER AT
C EACH WAVELENGTH INTERVAL.  THE STANDARD RELATIVE LUMINOSITY
C CURVE SHOULD BE USED FOR MOST APPLICATIONS (LUMENS/WATT).
21      REAL LEL
C VARIABLE LEL IS THE LUMINOUS EFFICIENCY OF THE LAMP (LUMENS/WATT).
22      REAL LT
C VARIABLE LT IS THE TOTAL LUMINOUS INTENSITY OF THE LAMP (LUMENS).
23      INTEGER M, N
C VARIABLES M AND N ARE COUNTERS USED IN VARIOUS DO-LOOPS THROUGH-
C OUT THE PROGRAM.
24      INTEGER NL
C VARIABLE NL IS THE NUMBER OF LAMPS BEING ANALYZED.
25      REAL PHI
C VARIABLE PHI IS THE VIEWING ANGLE OF THE SUBJECT, MEASURED
C RELATIVE TO THE SURFACE NORMAL (RADIANS).
26      REAL PI
C VARIABLE PI IS THE RATIO OF THE CIRCUMFERENCE OF A CIRCLE TO ITS
C DIAMETER (DIMENSIONLESS).
27      INTEGER RDIM
C VARIABLE RDIM IS THE LOCATION IN ARRAY X CONTAINING DISTANCE R2.
28      REAL RE
C VARIABLE RE IS THE REFLECTOR EFFICIENCY ASSUMED FOR EACH LAMP
C (0-1, DIMENSIONLESS).
```

```
29        REAL RT
   C VARIABLE RT IS THE DISTANCE FROM THE CAMERA TO THE SUBJECT (METERS).
30        REAL R1
   C VARIABLE R1 IS THE DISTANCE FROM THE CAMERA TO THE CLOSEST POINT
   C ALONG THE LINE OF SIGHT THAT IS ILLUMINATED BY THE LAMP (METERS).
31        REAL R2
   C VARIABLE R2 IS THE DISTANCE FROM THE CAMERA TO THE FARTHEST POINT
   C ALONG THE LINE OF SIGHT THAT IS ILLUMINATED BY THE LAMP (METERS).
32        REAL SIGMA
   C VARIABLE SIGMA IS THE VALUE OF THE VOLUME SCATTERING FUNCTION FOR
   C ALL BACKSCATTERING DIRECTIONS (ASSUMED CONSTANT IN THIS ANALYSIS).
   C (1/METER-STERADIAN).
33        REAL TBBT
   C VARIABLE TBBT IS THE COMPOSITE SUM OF BBT VALUES FOR ALL LAMPS
   C (LUMENS/STERADIAN-SQ METER).
34        REAL TBCT
   C VARIABLE TBCT IS THE COMPOSITE SUM OF BCT VALUES FOR ALL LAMPS
   C (LUMENS/STERADIAN-SQ METER).
35        REAL TBDT
   C VARIABLE TBDT IS THE COMPOSITE SUM OF BDT VALUES FOR ALL LAMPS
   C (LUMENS/STERADIAN-SQ METER).
36        REAL TC
   C VARIABLE TC IS THE COMPOSITE CONTRAST OF THE SUBJECT DUE TO ALL
   C LAMPS (DIMENSIONLESS).
37        INTEGER TDIM
   C VARIABLE TDIM IS THE LOCATION IN ARRAY X CONTAINING DISTANCE RT.
38        REAL TEB(30)
   C ARRAY TEB CONTAINS VALUES FOR THE SUBJECT RADIANCE AT THE LOCATION
   C OF THE CAMERA AT EACH WAVELENGTH INTERVAL DUE TO ALL LAMPS
   C (WATTS/STERADIAN-SQ METER-NANOMETER).
39        REAL TLEL
   C VARIABLE TLEL IS THE COMPOSITE LUMINOUS EFFICIENCY OF ALL LAMPS
   C (LUMENS/WATT).
40        REAL TLT
   C VARIABLE TLT IS THE COMPOSITE SUM OF LT VALUES FOR ALL LAMPS
   C (LUMENS).
41        REAL TWT
   C VARIABLE TWT IS THE COMPOSITE SUM OF WT VALUES FOR ALL LAMPS
   C (WATTS).
42        REAL WT
   C VARIABLE WT IS THE TOTAL ELECTRICAL POWER DRAWN BY THE LAMP
   C (WATTS).
43        REAL X(250)
   C ARRAY X CONTAINS DISTANCE VALUES FROM R1 TO R2 IN D METER INCRE-
   C MENTS (METERS).
   C INITIALIZE VARIABLES
```

```
      DO 2 N=1,30
      TEB(N)=0.0
    2 CONTINUE
      TBBT=0.0
      TBCT=0.0
      TBDT=0.0
      TLT=0.0
      TWT=0.0
C EVALUATE PI
      PI=3.141592654
C INPUT INCREMENT SIZE
      READ, D
      PRINT, D
C INPUT ENVIRONMENTAL DATA
      DO 5 N=1,30
      READ, A(N)
      PRINT, A(N)
    5 CONTINUE
      DO 10 N=1,30
      READ, K(N)
      PRINT, K(N)
   10 CONTINUE
      READ, SIGMA
      PRINT, SIGMA
C INPUT SUBJECT DATA
      READ, C3
      PRINT, C3
      READ, PHI
      PRINT, PHI
      READ, RT
      PRINT, RT
C INPUT RECEIVER DATA
      DO 15 N=1,30
      READ, LE(N)
      PRINT, LE(N)
   15 CONTINUE
C INPUT LIGHTING DATA
      READ, NL
      PRINT, NL
      DO 100 J=1,NL
      DO 20 N=1,30
      READ, I(N)
   20 CONTINUE
      WRITE (6,21) J
   21 FORMAT('0','ANALYSIS OF LAMP NUMBER:-',1X,I2)
      WRITE (6,998)
  998 FORMAT(' ','      //$DATA')
```

```
      DO 999 N=1,30
      PRINT, I(N)
  999 CONTINUE
      READ, WT
      PRINT, WT
      READ, B
      PRINT, B
      READ, RE
      PRINT, RE
      READ, R1
      PRINT, R1
      READ, R2
      PRINT, R2
      READ, L
      PRINT, L
C INITIALIZE VARIABLES
      BBT=0.0
      BCT=0.0
      BDT=0.0
      LT=0.0
C TEST LAMP GEOMETRY
      IF(RT.GT.R2) GO TO 22
      IF(R1.GT.RT) GO TO 22
      GO TO 24
   22 CONTINUE
      WRITE(6,23)
   23 FORMAT(' ','THIS LAMP DOES NOT ILLUMINATE SUBJECT.')
      GO TO 95
   24 CONTINUE
C BEGIN CALCULATIONS
      C1=(2.5-1.5*ALOG10(2.0*PI/B))*0.0795774715
      C2=7.0*SQRT(2.0*PI/B)*C1
      DO 25 N=1,30
      EA(N)=(I(N)/(L*L))*(EXP(-A(N)*L)+C1*K(N)*L*EXP(-K(N)*L)+
     XC2*K(N)*L*EXP(-K(N)*L*2.0))
      EB(N)=C3*0.3183098862*EA(N)*COS(PHI)*EXP(-A(N)*RT)
      BBT=BBT+10.0*EB(N)*LE(N)
      LT=LT+10.0*B*(1/RE)*I(N)*LE(N)
   25 CONTINUE
      LEL=LT/WT
      IF(R2-(R1+249*D)) 28,28,26
   26 CONTINUE
      WRITE(6,27)
   27 FORMAT(' ','INCREMENT D IS TOO SMALL.')
      GO TO 110
   28 CONTINUE
      DO 33 N=1,250
```

```
128         X(N)=R1+(N-1)*D
129         IF(ABS(RT-X(N)).LE.D/2) GO TO 31
130         GO TO 32
131      31 CONTINUE
132         IF(N.EQ.1) TDIM=N+1
133         IF(N.GT.1) TDIM=N
134      32 CONTINUE
135         IF(X(N).GE.R2) GO TO 34
136      33 CONTINUE
137      34 CONTINUE
138         RDIM=N
139      35 CONTINUE
140         DO 45 N=1,30
141         DO 40 M=1,RDIM
142         FX1(N,M)=EXP(-2.0*A(N)*X(M))/(X(M)**2)
143         FX2(N,M)=EXP(-1.0*(A(N)+K(N))*X(M))/X(M)
144         FX3(N,M)=EXP(-1.0*(A(N)+2.0*K(N))*X(M))/X(M)
145      40 CONTINUE
146         CALL INTZ(X,FX1,INT1,2,RDIM,N)
147         CALL INTZ(X,FX2,INT2,2,RDIM,N)
148         CALL INTZ(X,FX3,INT3,2,RDIM,N)
149         CALL INTZ(X,FX1,INT4,TDIM,RDIM,N)
150         CALL INTZ(X,FX2,INT5,TDIM,RDIM,N)
151         CALL INTZ(X,FX3,INT6,TDIM,RDIM,N)
152         EC(N)=SIGMA*I(N)*(INT1(N)+C1*K(N)*INT2(N)+C2*K(N)*INT3(N))
153         ED(N)=SIGMA*I(N)*(INT4(N)+C1*K(N)*INT5(N)+C2*K(N)*INT6(N))
154         BCT=BCT+10.0*EC(N)*LE(N)
155         BDT=BDT+10.0*ED(N)*LE(N)
156      45 CONTINUE
157         C=(BBT-BDT)/BCT
      C SUM UP CONTRIBUTIONS FROM EACH LAMP
158         DO 50 N=1,30
159         TEB(N)=TEB(N)+EB(N)
160      50 CONTINUE
161         TBBT=TBBT+BBT
162         TBCT=TBCT+BCT
163         TBDT=TBDT+BDT
164         TLT=TLT+LT
165         TWT=TWT+WT
      C OUTPUT RESULTS OF SINGLE LAMP ANALYSIS
166         WRITE(6,55)
167      55 FORMAT(' ','SUBJECT SPECTRAL RADIANCE AT THE LOCATION OF THE
           XCAMERA:-')
168         WRITE(6,60)
169      60 FORMAT(' ','WAVELENGTH(NM)   WATTS/SR-SQ M-NM')
170         WRITE(6,61) EB(1)
```

```
171    61 FORMAT(' ','   400-410   ',5X,F14.10)
172       WRITE(6,62) EB(2)
173    62 FORMAT(' ','   410-420   ',5X,F14.10)
174       WRITE(6,63) EB(3)
175    63 FORMAT(' ','   420-430   ',5X,F14.10)
176       WRITE(6,64) EB(4)
177    64 FORMAT(' ','   430-440   ',5X,F14.10)
178       WRITE(6,65) EB(5)
179    65 FORMAT(' ','   440-450   ',5X,F14.10)
180       WRITE(6,66) EB(6)
181    66 FORMAT(' ','   450-460   ',5X,F14.10)
182       WRITE(6,67) EB(7)
183    67 FORMAT(' ','   460-470   ',5X,F14.10)
184       WRITE(6,68) EB(8)
185    68 FORMAT(' ','   470-480   ',5X,F14.10)
186       WRITE(6,69) EB(9)
187    69 FORMAT(' ','   480-490   ',5X,F14.10)
188       WRITE(6,70) EB(10)
189    70 FORMAT(' ','   490-500   ',5X,F14.10)
190       WRITE(6,71) EB(11)
191    71 FORMAT(' ','   500-510   ',5X,F14.10)
192       WRITE(6,72) EB(12)
193    72 FORMAT(' ','   510-520   ',5X,F14.10)
194       WRITE(6,73) EB(13)
195    73 FORMAT(' ','   520-530   ',5X,F14.10)
196       WRITE(6,74) EB(14)
197    74 FORMAT(' ','   530-540   ',5X,F14.10)
198       WRITE(6,75) EB(15)
199    75 FORMAT(' ','   540-550   ',5X,F14.10)
200       WRITE(6,76) EB(16)
201    76 FORMAT(' ','   550-560   ',5X,F14.10)
202       WRITE(6,77) EB(17)
203    77 FORMAT(' ','   560-570   ',5X,F14.10)
204       WRITE(6,78) EB(18)
205    78 FORMAT(' ','   570-580   ',5X,F14.10)
206       WRITE(6,79) EB(19)
207    79 FORMAT(' ','   580-590   ',5X,F14.10)
208       WRITE(6,80) EB(20)
209    80 FORMAT(' ','   590-600   ',5X,F14.10)
210       WRITE(6,81) EB(21)
211    81 FORMAT(' ','   600-610   ',5X,F14.10)
212       WRITE(6,82) EB(22)
213    82 FORMAT(' ','   610-620   ',5X,F14.10)
214       WRITE(6,83) EB(23)
215    83 FORMAT(' ','   620-630   ',5X,F14.10)
216       WRITE(6,84) EB(24)
```

```
217    84 FORMAT(' ',' 630-640 ',5X,F14.10)
218       WRITE(6,85) EB(25)
219    85 FORMAT(' ',' 640-650 ',5X,F14.10)
220       WRITE(6,86) EB(26)
221    86 FORMAT(' ',' 650-660 ',5X,F14.10)
222       WRITE(6,87) EB(27)
223    87 FORMAT(' ',' 660-670 ',5X,F14.10)
224       WRITE(6,88) EB(28)
225    88 FORMAT(' ',' 670-680 ',5X,F14.10)
226       WRITE(6,89) EB(29)
227    89 FORMAT(' ',' 680-690 ',5X,F14.10)
228       WRITE(6,90) EB(30)
229    90 FORMAT(' ',' 690-700 ',5X,F14.10)
230       WRITE(6,91) BBT
231    91 FORMAT(' ','SUBJECT LUMINANCE AT CAMERA (LUMENS/SR-SQ M):-',
         X1X,F14.10)
232       WRITE(6,92) LEL
233    92 FORMAT(' ','LUMINOUS EFFICIENCY OF LAMP (LUMENS/WATT):-',
         X1X,F14.10)
234       WRITE(6,93) C
235    93 FORMAT(' ','SUBJECT CONTRAST:-',1X,F14.10)
236    95 CONTINUE
237   100 CONTINUE
    C OUTPUT RESULTS OF COMPOSITE ANALYSIS.
238       WRITE(6,105)
239   105 FORMAT('0','COMPOSITE ANALYSIS.')
240       WRITE(6,55)
241       WRITE(6,60)
242       WRITE(6,61) TEB(1)
243       WRITE(6,62) TEB(2)
244       WRITE(6,63) TEB(3)
245       WRITE(6,64) TEB(4)
246       WRITE(6,65) TEB(5)
247       WRITE(6,66) TEB(6)
248       WRITE(6,67) TEB(7)
249       WRITE(6,68) TEB(8)
250       WRITE(6,69) TEB(9)
251       WRITE(6,70) TEB(10)
252       WRITE(6,71) TEB(11)
253       WRITE(6,72) TEB(12)
254       WRITE(6,73) TEB(13)
255       WRITE(6,74) TEB(14)
256       WRITE(6,75) TEB(15)
257       WRITE(6,76) TEB(16)
258       WRITE(6,77) TEB(17)
259       WRITE(6,78) TEB(18)
```

```
      WRITE(6,79) TEB(19)
      WRITE(6,80) TEB(20)
      WRITE(6,81) TEB(21)
      WRITE(6,82) TEB(22)
      WRITE(6,83) TEB(23)
      WRITE(6,84) TEB(24)
      WRITE(6,85) TEB(25)
      WRITE(6,86) TEB(26)
      WRITE(6,87) TEB(27)
      WRITE(6,88) TEB(28)
      WRITE(6,89) TEB(29)
      WRITE(6,90) TEB(30)
      WRITE(6,91) TBBT
      TLEL=TLT/TWT
      WRITE(6,92) TLEL
      TC=(TBBT-TBDT)/TBCT
      WRITE(6,93) TC
  110 CONTINUE
      RETURN
      END

      SUBROUTINE INTZ(XX,YY,ZZ,LL,UL,R)
      REAL SUM
      REAL XX(250)
      REAL YY(30,250)
      REAL ZZ(30)
      INTEGER Q, R, LL, UL
      SUM=0.0
    1 DO 2 Q=LL,UL
      SUM=SUM+0.5*(XX(Q)-XX(Q-1))*(YY(R,Q)+YY(R,Q-1))
    2 CONTINUE
    3 ZZ(R)=SUM
      RETURN
      END
//$DATA
(INSERT DATA DECK HERE)
/*
```